

CHARACTERISATION OF LOCAL GRAIN SIZE VARIATION OF WELDED STRUCTURAL STEEL

KARAKTERIZACIJA PROMENE LOKALNE VELIČINE ZRNA NA ZAVARENIM KONSTRUKCIONIM ČELICIMA

Originalni naučni rad / Original scientific paper

UDK / UDC: Weld World (2014) 58:491–497;

DOI 10.1007/s40194-014-0132-0

Rad primljen / Paper received:

Septembar 2016.

Adresa autora / Author's adresse :

* Pauli Lehto pauli.lehto@aalto.fi

¹ Department of Mechanical Engineering, School of Engineering, Aalto University, P.O. Box 12200, FIN-00076 Aalto, Finland

Prevod izvornog rada na srpski jezik: Milica Antić, dipl.ing

Key words: Grain size. Measurement. Structural steels. Hardness. Microstructure. Weld metal

Ključne reči: Veličina zrna. Merenje. Konstrukcioni čelik. Tvrdća. Mikrostruktura. Metal šava

Abstract

Previously, it has been shown that the grain size distribution plays an important role in the mechanical properties of welded steel. In the previous investigation, the volume-weighted average grain size has been shown to capture the influence of grain size distribution, resulting in a better fitting Hall–Petch relationship between grain size and hardness. However, the previous studies exclude the effects arising from local variation in grain size. In this paper, the grain size measurement methods are extended for the characterisation of the local grain size variation, which is significant for welded joints and can have an adverse effect on mechanical properties.

The local gradient of grain size variation and its dependency on measurement direction are considered. In addition, examples of grain size and hardness variation are shown for S355 base metal and two weld metals, and characteristic differences are highlighted and discussed. The coarse-grained areas of a heterogeneous microstructure are found to have lower hardness than fine-grained areas. However, the surrounding microstructure, i.e. local grain size gradient, has an influence on the measured hardness values.

1 Introduction

Microstructural characterisation of engineering materials is a necessity for understanding the relationships between microstructural quantities and mechanical properties. Grain size is one of the fundamental microstructural quantities and correlates with several properties, such as hardness, stress–strain curve and fatigue strength [1–7]. Based on the work of Hall [8] and Petch [9], a relationship was found between grain size and the

Rezime

Ranije je pokazano da distribucija veličine zrna igra važnu ulogu vezanu za mehanička svojstva zavarenog čelika. U prethodnom istraživanju, zapreminski procenjena prosečna veličina zrna je pokazala uticaj distribucije veličine zrna, što je rezultovalo u boljem ispunjenju Hall-Petch-og odnosa između veličine zrna i tvrdoće. Međutim, prethodne studije isključuju učinke koji proizlaze iz lokalnih varijacija u veličini zrna. U ovom radu, metode merenja veličine zrna su proširene na karakterizaciju varijacije lokalne veličine zrna, što je značajno za zavarene spojeve jer mogu imati negativan uticaj na mehanička svojstva.

Razmatraju se lokalni gradijent varijacije veličine zrna i njegova zavisnost od smera merenja. Osim toga, primeri veličine zrna i varijacije tvrdoće su prikazani za S355 kao osnovni materijal i dva šava metala, a karakteristične razlike su istaknute i o njima se diskutuje. Za područja krupnozrne heterogene mikrostrukture utvrđeno je da imaju manju tvrdoću od sitnozrnog područja. Međutim, okružujuća mikrostruktura, t.j. gradijent lokalne veličine zrna, ima uticaj na izmerene vrednosti tvrdoće.

1. Uvod

Mikrostrukturna karakterizacija inženjerskih materijala je neophodna za razumevanje odnosa između mikrostrukturnih veličina i mehaničkih svojstava. Veličina zrna je jedna od osnovnih mikrostrukturnih veličina i u korelaciji je sa nekoliko svojstava, kao što su tvrdoća, kriva naprezanje-deformacija i zamorna čvrstoća [1-7]. Zasnovan na radu Hall [8] i Petch [9], pronađen je odnos između

mechanical properties of steel. For yield strength, this relationship is:

$$\sigma = \sigma_0 + kd^{-1/2} \quad (1)$$

where σ_0 is the lattice friction stress required to move individual dislocations, k is a material-dependent constant known as the Hall–Petch slope, and d is the average grain size [10]. As the Hall–Petch relationship is related to the measure of grain size, the correct definition of grain size is crucial. The most commonly reported microstructural measure in literature is the average grain, even though there is a large variety of, e.g. ASTM grain size measurement methods, available [11]. Moreover, orientation imaging microscopy gives the operator a large degree of freedom for defining the measurement methodology and parameters such as step size, grain boundary misorientation criteria and filtering of the data [12–14]. For these reasons, an extensive interlaboratory round-robin [15] was carried out in order to define the grain size measurement methodology for the ISO 13067 [16] standard. In addition to measurement of average grain size, other material-specific factors such as differences in phase structure and grain size distribution need to be considered. For heterogeneous materials, the grain size distribution is of particular interest since it has been shown to influence the mechanical properties [10, 17–22]. Improved grain size measurement methods are thus required to enhance the understanding between grain size distribution and mechanical properties [11]. Accurate description of the microstructural heterogeneity is also required for the mesoscale modelling of material behaviour [12]. Welds are an extreme case of heterogeneity since it is present both in macroscopic scale across the joint and in microscopic scale within a single zone; see Fig. 1. The grain size characterisation of heterogeneous weld metals was studied by Lehto et al. [23]. The grain size measurements revealed that structural steel weld metals exhibit a large variety of grain size distributions that are noticeably broader than those of the base metal. To capture the influence of grain size distribution, the volume-weighted grain size measurement was utilised. It was shown that the Hall–Petch relationship's dependence on grain size distribution is eliminated when then volume-weighted average grain size (d_v) is used:

$$\sigma = \sigma_0 + kd_v^{-1/2} = \sigma_0 + kd_v^{-1/2} \left(1 + f \frac{\Delta d}{d}\right), \quad (2)$$

veličine zrna i mehaničkih svojstava čelika. Za napon tečenja, ovaj odnos je:

gde je σ_0 napon trenja rešetke potreban za kretanje pojedinačnih dislokacija, k je konstanta zavisna od materijala poznata kao Hall-Petch nagib, a d je prosečna veličina zrna [10]. Kako je Hall-Petch odnos vezan za meru veličine zrna, ispravna definicija veličine zrna je od ključnog značaja. Najčešće saopštavana mikrostrukturalna mera u literaturi je prosečna veličina zrna, iako postoji veliki izbor metoda na raspolaganju, npr ASTM metoda merenja veličine zrne [11]. Osim toga, mikroskopija sa orijentacijom slike, daje operateru veliki stepen slobode za definisanje metodologije merenja i parametara kao što su veličina koraka, kriterijumi neorijentisanosti granica zrna i filtriranje podataka [12-14]. Iz tih razloga, sprovedena su opsežna međulaboratorijska ispitivanja [15] kako bi se definisala metodologija merenja veličine zrna za ISO standard 13067 [16]. Uz merenje prosečne veličine zrna, druge faktore specifične za materijal, kao što su razlike u strukturnim fazama i distribucija veličine zrna, treba uzeti u obzir.

Kod heterogenih materijala, distribucija veličine zrna je od posebnog interesa jer se pokazalo da utiče na mehanička svojstva [10, 17-22]. Poboljšane metode merenja veličine zrna traže da se poboljša razumevanje između distribucije veličine zrna i mehaničkih svojstava [11]. Precizan opis mikrostrukturnih heterogenosti je takođe potreban za međuskalno modeliranje ponašanje materijala [12]. Zavareni spojevi su ekstremni slučaj heterogenosti jer je ona prisutna i u makroskopskoj skali i na mikroskopskom nivou unutar jedne zone; vidi sl. 1. Karakterizacija veličine zrna heterogenih metala šava su proučavali Lehto i dr. [23]. Merenja veličine zrna su pokazala da metali šava od konstrukcionih čelika pokazuju veliki izbor distribucije veličine zrna koji je znatno veći od onih osnovnog materijala. Da bi se snimio uticaj distribucije veličine zrna, merenje veličine naglašenog zrna se koristi. Pokazano je da se zavisnost Hall-Petch odnosa od distribucije veličine zrna ne može primeniti a kada se koristi zapreminski procenjena prosečna veličina zrna (d_v) onda je:

where f is a constant describing the relation between average and volume-weighted average grain size and $\Delta d/d$ is the relative grain size dispersion. The equation is reduced to the original Hall–Petch Eq. (1) in the theoretical case that all grains are the same size. Furthermore, if samples with similar grain size dispersion are compared the original Hall–Petch, Eq (1) is applicable.

While the previous work covered the microstructural characterisation of volume-weighted average grain size and its relation to the grain size distribution of welded structural steel, it did not provide further insight into the inherent large local variation of grain size. The aim of this paper is to characterise the local variation of grain size in welded joints and investigate how it influences the mechanical properties using hardness measurements. The point-sampled grain size measurement method is extended for the characterisation of local grain size variation both in numerical and visual form. The numerical approach is to present a moving average of grain size using line probes in different directions. In visual approach, the characterisation of grain size variation is further developed by substituting grain size (d) with the Hall–Petch grain size parameter ($d-0.5$) in order to have a linear scale for grain sizedependent mechanical properties. The local variation of grain size is also compared to hardness measurement results.

2. Measurement of local grain size variation

Grain size is measured using the point-sampled intercept length method [24, 25]. The method is similar to the commonly used linear intercept method [26]; however, the measurements are carried out at random points instead of being measured along pre-determined lines. The method has previously been used for the characterisation of grain size distribution in welded structural steel [23]. Here, the method is extended for the characterisation of local grain size variation by including measurement direction-based averaging. In addition, moving averages of grain size are calculated across the microstructure. Figure 2 shows a flow chart of the measurement procedure using a fictional single-phase microstructure. Firstly, the grain size is measured for individual grains at random points that hit the grain interior (Fig. 2 (1a)). The procedure is repeated a large number of times for one measurement direction, resulting in densely measured grain size for the individual grain (Fig. 2 (1b)).

gde je f konstanta koja opisuje odnos između srednje vrednosti i zapreminski procenjene veličine zrna i $\Delta d / d$ je relativna disperzija veličina zrna. Jednačina se svodi na originalnu Hall-Petch jedn. (1) u teorijskom slučaju da su sva zrna iste veličine. Osim toga, ako se uzorci sa sličnom disperzijom veličine zrna su u odnosu na originalni Hall-Petch, jednačina (1) je na snazi.

Dok je dosadašnji rad pokrivaio mikrostrukturnu karakterizaciju zapreminski procenjene prosečne veličine zrna i njen odnos prema distribuciji veličine zrna kod zavarenih konstrukcionih čelika, nije pružio dublji uvid u unutrašnje velike lokalne varijacije veličine zrna. Cilj ovog rada je da se okarakterišu lokalne varijacije veličine zrna kod zavarenih spojeva i istraživanje kako utiču na mehaničke osobine korišćenjem merenja tvrdoće. Metoda merenja tačkastim uzorkovanjem je proširena na karakterizaciju varijacija lokalne veličine zrna kako u numeričkom tako i u vizuelnom obliku. Numerički pristup je da predstavi kretanje prosečne veličine zrna korišćenjem linijskih sondi u različitim pravcima. Kod vizuelnog pristupa, karakterizacija varijacije veličine zrna se dalje razvija zamenom veličine zrna (D) sa parametrom veličine zrna Hall-Petch ($d-0,5$) da bi se dobila linearna skala za mehanička svojstva zavisna od veličine zrna. Lokalna varijacija veličine zrna je takođe upoređena sa rezultatima merenja tvrdoće.

2. Merenje varijacije lokalne veličine zrna

Veličina zrna se meri metodom tačkastog uzorkovanja prekinutih dužina [24, 25]. Metoda je slična najčešće korišćenoj linearnoj prekidnoj metodi [26]; međutim, merenja se obavljaju na slučajnim tačkama umesto da se mere po unapred određenim linijama. Metoda je prethodno korišćena za karakterizaciju distribucije veličine zrna na zavarenim čeličnim konstrukcijama [23]. Ovde je metoda proširena na karakterizaciju varijacije veličine lokalnih zrna uključujući merenja na bazi usmerenog preseka. Osim toga, kretanja prosečnih veličina zrna se obračunavaju preko mikrostrukture. Slika 2 prikazuje dijagram toka postupka merenja korišćenjem izmišljene jednofazne mikrostrukture. Prvo, veličina zrna se meri za pojedinačna zrna u nasumičnim tačkama koje su pogodile unutrašnjost zrna (Sl. 2 (1a)). Postupak se ponavlja veliki broj puta za jedan smer merenja, što je rezultiralo u gusto merenim veličinama zrna za pojedinačna zrna (Sl. 2 (1b)).

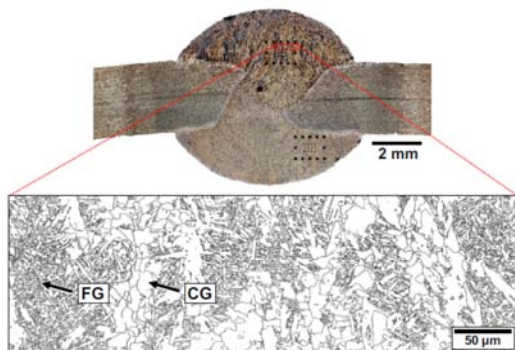
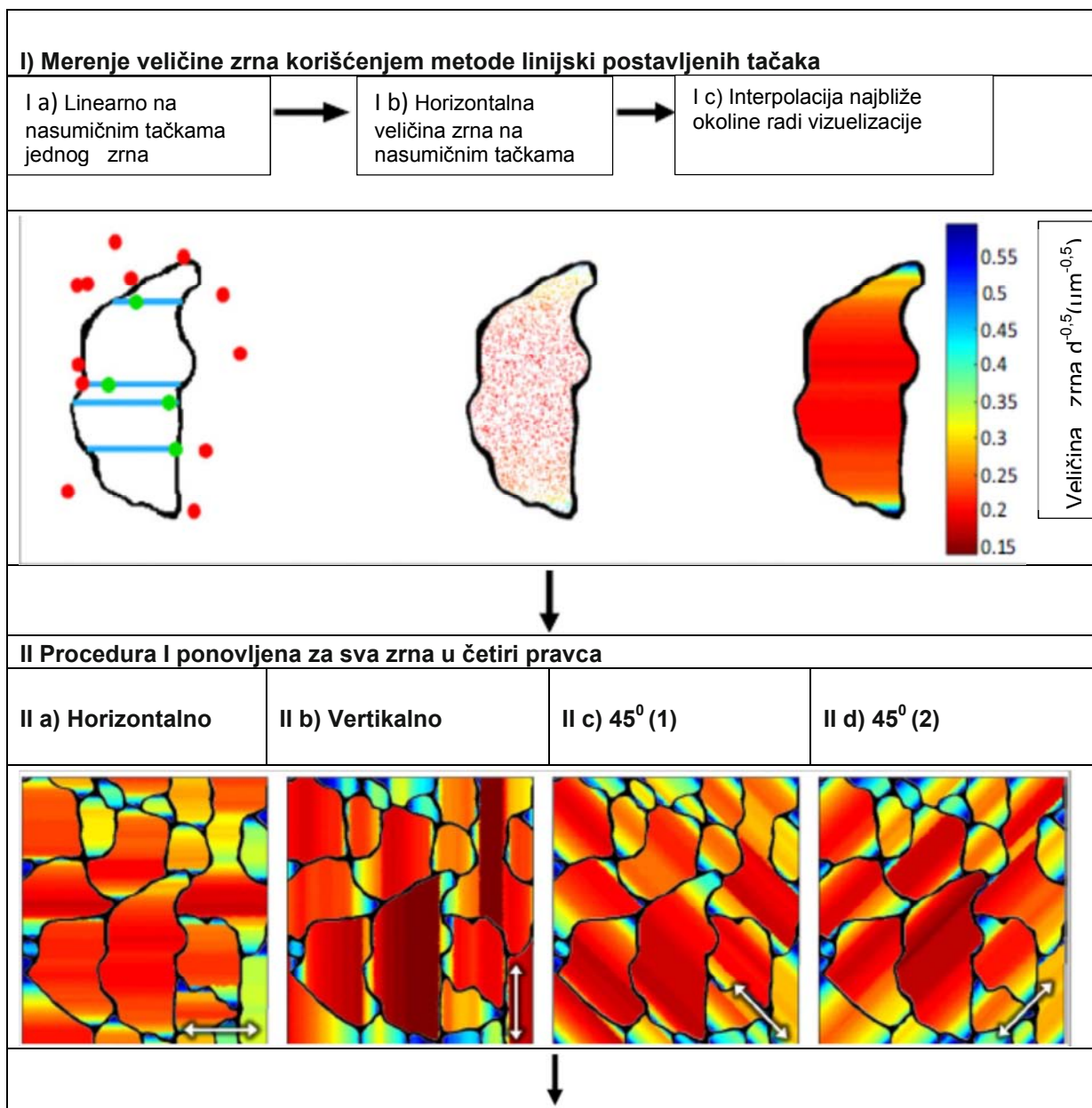


Fig. 1 Macro section of an arc welded joint (CV.1) and an example of weld metal grain size variation showing fine grained (FG) and coarse grained (CG) areas

Sl. 1. Makro presek elektroločno zavarenog spoja (CV1) i primer varijacije veličine zrna metala šava pokazujući oblasti finog zrna (FG) i grubog zrna (CG)



III Kombinacija četiri pravca merenja		
III a) Minimum	III b) Srednja vrednost	III c) Maksimum

Fig. 2 Flowchart of the grain size measurement and analysis procedure

Sl. 2 Dijagram toka merenja veličine zrna i postupak analize

For an improved visual representation, the non-measured points are filled with a value from the nearest neighbouring point. As shown in (Fig. 2 (Ic)), the interpolation results in a good visual representation of grain size for the individual grain. Grain size is presented using the Hall–Petch grain size parameter ($d^{-0.5}$) in order to have a linear scale for grain size affected mechanical properties. This approach is taken to improve the resolution of visual representation in the grain size regime below $10\ \mu\text{m}$. Based on the Hall–Petch relationship, a small change of grain size in this regime has a significant effect on the mechanical properties, e.g. strength doubles as grain size decreases from 4 to $1\ \mu\text{m}$.; see Fig. 3. It is noted that the classical Hall–Petch relationship is applicable at grain sizes larger than $0.1\ \mu\text{m}$ ($d^{-0.5} < 3.16\ \mu\text{m}^{-0.5}$) [27, 28].

Za poboljšanje vizuelnog predstavljanja, za neizmerene tačke se ispunjava vrednošću najbliže susedne tačke. Kao što je prikazano (Sl. 2 (Ic)), rezultati interpolacije su dobar vizuelni prikaz veličine zrna za pojedinačna zrna. Veličina zrna je predstavljena Hall-Petch parametrom veličine zrna ($d^{-0,5}$) kako bi se dobila linearna skala veličine zrna koja utiče na mehanička svojstva. Ovaj pristup se uzima za poboljšanje rezolucije vizuelne prezentacije u opsegu veličine zrna ispod $10\ \mu\text{m}$. Na bazi Hall-Petch odnosa, mala promena veličine zrna u ovom režimu ima značajan uticaj na mehanička svojstva, npr. čvrstoća se duplira ako se veličina zrna smanjuje od 4 do $1\ \mu\text{m}$.; vidi sliku. 3. Napominje se da je klasični Hall-Petch odnos primerljiv za zrna veća od $0,1\ \mu\text{m}$ ($D-0.5 < 3.16\ \mu\text{m}-0.5$) [27, 28].

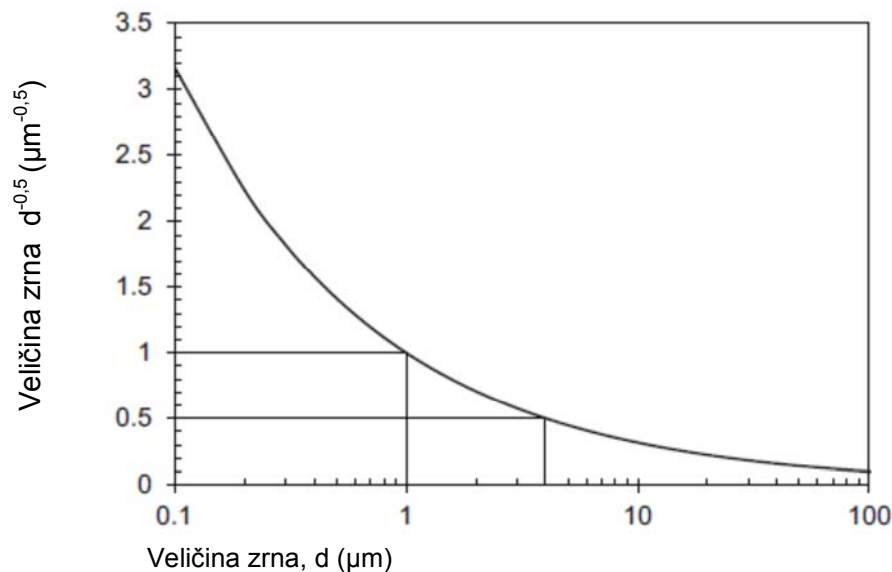


Fig. 3 Relationship between grain size (d) and the Hall–Petch grain size parameter ($d^{-0.5}$)

Sl. 3 Međusobni odnos između veličine zrna (d) i Hall–Petch parametra veličine zrna ($d^{-0.5}$)

The procedures (Fig. 2 (Ia–c)) are repeated for all grains in the fictitious microstructure using four measurement directions (0°, 45°, 90°, and 135°) as shown in Fig. 2 (IIa–d). Typically, at least 25 % of the image points should be measured in each direction for accurate results. The probability P_i of a random point hitting a grain of size i is proportional to the surface area fraction of the grain. Based on relationships of stereology [29, 30], the surface area fraction provides a statistical estimator for the volume fraction: $P_i \approx \frac{1}{4} \frac{A_i}{A_t}$

$$P_i = \frac{A_i}{A_t} \approx \frac{V_i}{V_t} \quad (3)$$

where A_i and V_i are the surface area and volume of a grain of size i . A_t and V_t are the total surface area and volume of all grains in the measurement domain, correspondingly. Thus, the measured grain size distribution can be considered as the volume-weighted grain size distribution if the assumption of isotropy is made. For further details and a Matlab implementation of the measurement procedure, the reader is referred to [23, 31]. To verify that the nearest neighbour interpolation does not introduce any bias or error to the data, the grain size distributions of the measured and interpolated data are compared in Fig. 4a. As the two counterparts overlap for each individual measurement direction, the interpolated data shown in (Fig. 2 (IIa–d)) can be used for further data analysis. In order to compare grain size with mechanical properties, e.g. hardness, the four measurement directions need to be combined into a single visualisation. The three alternatives used are to take the minimum, mean or maximum value of the four measurement directions at each point of all grains; see in Fig. 2 (IIIa–c). As shown in Fig. 4b, the grain size distributions of minimum and maximum cases are the lower and upper bounds for the measurement data, respectively. The mean has closely the same volume weighted The procedures (Fig. 2 (Ia–c)) are repeated for all grains in the fictitious microstructure using four measurement directions (0°, 45°, 90°, and 135°) as shown in Fig. 2 (IIa–d). The mean has closely the same volumeweighted average grain size, d_v , as the measurement data even though the shape of the distribution is different. The agreement of volume-weighted average grain size has been verified for various heterogeneous microstructures, with the error typically being smaller than 1 %. Since the volume-weighted average grain size has been shown to correlate with hardness according to the Hall–Petch relationship [23], the mean grain size plot is used for further result analysis of hardness and grain size. In addition to the above

Procedure (Sl. 2 (Ia-c)) se ponavljaju za sva zrna fiktivne mikrostrukture koristeći četiri smjera merenja (0°, 45°, 90°, i 135°) kao što je prikazano na slici 2 (IIa-d). Tipično, najmanje 25% tačaka na slici treba meriti u svakom smeru za precizne rezultate. Verovatnoća P_i nasumične tačke da se pogodi veličina zrna, proporcionalna je površini frakcija zrna. Na bazi stereoloških odnosa [29, 30], površina frakcije pruža statističke procene za zapreminu frakcije.

gde su A_i i V_i površina i zapremina zrna veličine i . A_t i V_t su ukupne površine i zapremine svih zrna u mernom domenu. Dakle, izmerena distribucija veličine zrna može se smatrati distribucijom veličine zapreminski procenjenih zrna uz pretpostavku izotropije. Za više detalja i implementacija Matlab postupka merenja, čitalac se upućuje na [23, 31]. Da bi se potvrdilo da interpolacija najbliže oblasti ne uvodi nikakve predrasude ili greške u podacima, upoređene su izmerene distribucije veličine zrna i interpolirani podaci na sl. 4a. S obzirom na preklapanje za svaki pojedini smer merenja, interpolirani podaci prikazani u (Sl. 2(IIa-D)) se mogu koristiti za dalju analizu podataka. Kako bi se uporedila veličina zrna sa mehaničkim svojstvima, npr tvrdoća, treba kombinovati četiri pravca merenja u jednu vizualizaciju. Tri alternative se koriste: da se odredi minimalna, srednja ili maksimalna vrednost u nekom od četiri pravca merenja u svakoj tački svih zrna; vidi na slici 2 (IIIa-c). Kao što je prikazano na sl. 4b, distribucija veličine zrna za minimalne i maksimalne slučajeve su donje i gornje granice za podatke merenja. Srednja vrednost je bliska onoj dobijenoj procedurom zapreminske procene. Procedure (sl. 2 (Ia-c)) se ponavljaju za sva zrna u fiktivnoj mikrostrukтури koristeći četiri smjera merenja (0°, 45°, 90°, i 135°) kao što je prikazano na slici 2(IIa-d). Srednja je bliska istoj zapreminski procenjenoj veličina zrna, d_v , kao podatak merenja iako je oblik distribucije drugačiji. Slaganje zapreminski procenjene srednje vrednosti veličine zrna, potvrđena je za različite heterogene mikrostrukture s tim da su greške obično manje od 1%. Dok je zapreminski procenjena srednja veličina zrna pokazala korelaciju sa tvrdoćom prema Hall-Petchovoj jednačini (23), prikaz srednje veličine se koristi za naredne analize rezultata tvrdoće i veličine zrna. Pored navedenih vizuelnih opcija, pokretni proseci minimalne, srednje i maksimalne konture veličine zrna (sl. 2 (IIIa-c)) se obračunavaju preko

mentioned visual options, the moving averages of the minimum, mean and maximum grain size contours (Fig. 2 (IIIa–c)) are calculated across the micrograph using horizontal and vertical line probes. The line probes used in this study are 10-pixel wide. In addition, the border regions of the micrographs were excluded from the averaging to eliminate large grains that extend beyond the micrograph. Grain size at 90 % probability level was found as a suitable margin for exclusion at all edges of the image. Dimensions of the probes used are shown in Table 3. The difference between the three moving averages represents the local variation of grain size in different measurement directions.

3 Experiments

3.1 Test specimens and sample preparation

The experiments are carried out for one base metal (BM.1) and two welded samples. The weld samples are flux-core arc welded either from two sides (CV.1) or from one side with a ceramic backing (CV.2). Plate edges were prepared by plasma cutting followed by grinding. The energy input for CV.1 is 3.5 kJ/cm for each side and for CV.2 it is 9 kJ/cm for the single weld bead. The macro sections of the weld samples CV.1 and CV.2 are shown in Figs. 1 and 5, correspondingly. All base metals are S355 grade ferritic-pearlitic structural steels; the base metal grades and mechanical properties are presented in Table 1.

mikrografija pomoću horizontalnih i vertikalnih linijskih sondi. Linijske sonde korišćene u ovoj studiji su širine 10-piksela. Osim toga, granične regije mikrografija su isključene iz proseka za otklanjanje velikih zrna koje se protežu radi eliminacije mikrografije. Veličine zrna na 90% nivou verovatnoće su se pokazale kao prikladan prostor za isključenje svih rubova slike. Dimenzije sondi koje su korišćene, prikazane su u tabeli 3. Razlika između tri pokretna proseka predstavlja lokalne varijacije veličine zrna u različitim pravcima merenja.

3. Eksperimenti

3.1. Epruvete za ispitivanje i priprema uzoraka

Eksperimenti su izvedeni na jednom osnovnom materijalu (BM.1) i dva zavarena uzorka. Uzorci šava su zavareni punjenom žicom ili obostrano (CV.1) ili sa jedne strane sa keramičkom podlogom (CV.2). Ivce lima su pripremljene plazma rezanjem a zatim brušenjem. Količina unete energije za CV.1 je 3,5 kJ / cm za obe strane i za CV.2 je 9 kJ / cm za jednostrani šav. Makropreseki uzoraka šava CV.1 i CV.2 prikazani su na slikama 1 i 5. Svi osnovni materijali su S355 klase feritno-perlitnih konstrukcionih čelika; klase osnovnog materijala i mehaničke karakteristike prikazane su u tabeli 1.

	Grade	Thickness (mm)	R _{eH} (MPa)	R _m (MPa)	A (%)
BM.1	GL D36	6	343	472	34
CV.1	S355J2	3	466	564	31,3
CV.2	S355J2	3	466	564	31,3

Table 1. Test sample base metal grades and mechanical properties [23]

	Klasa	Debljina (mm)	R _{eH} (MPa)	R _m (MPa)	A (%)
BM.1	GL D36	6	343	472	34
CV.1	S355J2	3	466	564	31,3
CV.2	S355J2	3	466	564	31,3

Tabela 1. Klase ispitnih uzoraka osnovnog materijala i mehaničke osobine [23]

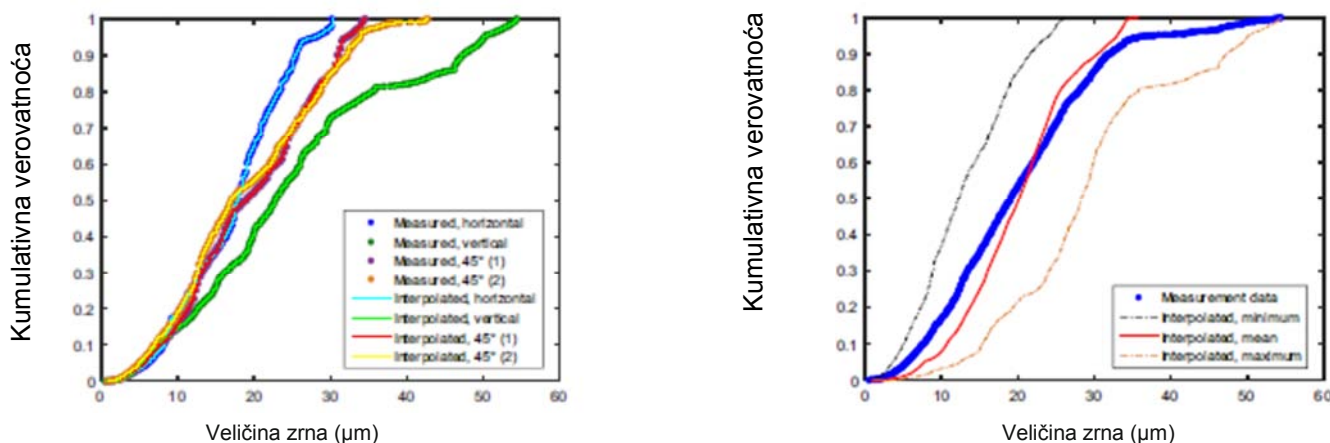


Fig. 4 Cumulative probability distributions for grain size (a) measured and interpolated data for the four measurement directions (see Ib, Ic and II in Fig. 2). b Comparison of the analysed (see III in Fig. 2) and measurement data

Sl. 4. Raspodela kumulativne verovatnoće za veličinu zrna (a) mereni i interpolirani podaci za četiri pravca merenja (videti Ib, Ic i II na sl.2). b) Upoređenje analiziranog (videti III na sl.2) i podaci merenja

	Sample	Grain size d_v (μm)	Hardness HM (MPa)	Constituent volume fraction (%)		
				AF	PF	FC/P
Base metal	BM.1	15,29±1,96	1412±29	-	78,6±53	21,4±5,3 (P)
Homogeneous weld metal	CV.1 root	5,95±0,20	1756±17	7,3±1,4	78,7±4,7	14,0±3,4
Heterogeneous weld metal	CV.2 toe	4,00±0,45	1984±34	37,5±6,4	56,2±53	6,3±1,6

Abbreviations used: d_v , volume-weighted average grain size, HM Martens hardness, PF primary ferrite, AC acicular ferrite, FC ferrite-carbide aggregate, P pearlite [23]

Table 2. Test specimen nomenclature, microstructural characterization and the microstructural constituent volume fractions and the corresponding 95% confidence intervals [23]

	Uzorak	Veličina zrna d_v (μm)	Tvrdća HM (MPa)	Zapreminski udeo konstituenata (%)		
				AF	PF	FC/P
Osnovni materijal	BM.1	15,29±1,96	1412±29	-	78,6±53	21,4±5,3 (P)
Homogeni metal šava	CV.1 koren	5,95±0,20	1756±17	7,3±1,4	78,7±4,7	14,0±3,4
Heterogeni metal šava	CV.2 podnožje	4,00±0,45	1984±34	37,5±6,4	56,2±53	6,3±1,6

Korišćene skraćenice: d_v , zapreminski određeni prosek veličine zrna, HM tvrdoća po Martensu, PF primarni ferit, AC acirkularni ferit, FC agregati ferit-karbida, P perlit [23]

Tabela 2. Nomenklatura ispitnih epruveta, mikrostrukturna karakterizacija i zapreminske frakcije mikrostrukturnih konstituenata i odgovarajući intervali usaglašenosti 95% [23]

For this investigation, specimens are prepared from the base metal BM.1 and the two weld metals. To represent the extremities of the grain size distribution, two weld metal regions are chosen with homogeneous and heterogeneous grain size distributions. The root side weld metal of weld sample CV.1 is taken as the homogeneous weld metal, while the toe side weld metal of weld sample CV.2 is the heterogeneous weld metal. The three specimens are chosen since they have previously been found to closely follow the same relationship between grain size and hardness in the macroscopic scale using 70–100 μm hardness

Za ovo istraživanje, uzorci su pripremljeni od osnovnih metala BM.1 i dva metala šava. Da bi predstavljali ekstremite distribucije veličine zrna, dve regije šava biraju se sa homogenom i heterogenom distribucijom veličine zrna. Korena strana metala šava uzorka CV.1 se uzima kao homogeni metal šava, dok je podnožje na strani metala šava uzorka CV.2 heterogeni šav. Tri uzorka su izabrana jer je prethodno utvrđeno da pažljivo prate isti odnos između veličine zrna i tvrdoće na makroskopskoj skali pomoću 70-100 μm rastojanja otisaka [23].

indentations [23]. The previously measured average hardness and grain size values, as well as phase volume fractions are presented in Table 2. The microstructural constituents were identified according to IIW document IX-1533-88 [32] by using the systematic manual point counting method according to ASTM E562-02 [33]. For the weld sample CV.2, an additional sample was prepared for EBSD analysis. The sample is used for comparing the grain size and hardness from the exact same location for the heterogeneous weld metal. This location is referred to as A2 in further instances. The location of this area and the hardness measurements carried out for the heterogeneous weld metal are shown in Fig. 5. All specimens were mounted in an electrically conductive resin and grinded up to P4000 grit abrasive paper. Polishing was done with 3 and 1 μm diamond paste and the additional heterogeneous sample with 0.25 μm as well. Before EBSD analysis, final polishing was carried out with colloidal silica in a vibratory polisher for 45 min.

3.2 Material characterisation

Instrumented indentation testing was used for measuring the mechanical properties. Hardness was measured with a CSM Instruments micro-indentation tester according to ISO 14577-1 [34] utilising large matrices containing up to 200 indentations. Hardness was defined using Martens hardness, denoted by HM, with a Vickers pyramid tip. The measurement data related to, but not presented in [23], indicates that HM correlates well with traditional Vickers hardness when presented in the same units; see Appendix 1 for further details. The test forces used equal HV0.01 (98.07 mN), HV0.1 (980.7 mN) and HV0.3 (2942.1 mN), producing indentations with approximately 7–10 μm , 30–35 μm and 50–60 μm diagonal lengths, respectively, depending on the sample. Indentation depth is approximately 1/7th of the indentation diagonal, i.e. 1–1.4 μm , 4.3–5 μm and 7.1–8.5 μm for the three measurement forces, respectively. Linear 30-s loading ramps were used, with a hold time of 10 s at the maximum force. The heterogeneous microstructure was characterised using the electron backscatter diffraction (EBSD). EBSD analysis of the heterogeneous weld metal in sample CV.2 (location A2) was carried out prior to hardness measurements at a premarked area. A Zeiss Ultra 55 field emission scanning electron microscope equipped with a Nordlys F+ camera and Channel 5 software from Oxford Instruments was used for the EBSD analyses. The EBSD analyses were performed with a step

Prethodno izmerene prosečne vrednosti tvrdoća i veličine, kao i zapreminske frakcije faza prikazane su u tabeli 2. Mikrostrukturni sastojci su identifikovani prema IIW dokument IX-1533-88 [32] pomoću sistematske metode ručnog prebrojavanja prema ASTM E562-02 [33]. Za uzorak šava CV.2, dodatni uzorak je pripremljen za analizu EBSD. Uzorak se koristi za poređenje veličine zrna i tvrdoće iz iste lokacije za heterogene šavove. Ova lokacija se naziva A2 u daljim razmatranjima.

Lokacija ovog područja i vrednosti tvrdoća za heterogene šavove su prikazani na slici. 5. Svi uzorci su postavljeni (zatopljeni) u elektroprovodljivu smolu i brušeni do P4000 granulacije brusnog papira. Poliranje je učinjeno sa dijamantskom pastom 3 i 1 μm a za dodatne heterogene uzorke sa 0,25 μm . Pre analize EBSD, završno poliranje izvršeno je sa koloidnim silikonom u uređaju za vibraciono poliranje za 45 min.

3.2 Karakterizacija materijala

Instrumentovano pomeranje pri ispitivanju korišćeno je za merenje mehaničkih svojstava. Tvrdoća je merena CSM Instruments mikro-ispitivačem prema ISO 14577-1 [34] koji koriste koriste velike matrice sa do 200 otisaka. Tvrdoća je definisana pomoću tvrdoće po Martensu, označen sa HM, sa vrhom Vickers piramide. Podaci merenja vezani za to, ali nisu predstavljeni u [23], ukazuju na dobru korelaciju HM sa tradicionalnom tvrdoćom po Vickersu kada su u istim jedinicama; vidi Dodatak 1 za više detalja. Sile pri ispitivanju su za HV0.01 (98.07 mN), HV0.1 (980,7 mN) i HV 0.3 (2942,1 mN), proizvode otiske sa oko 7-10 μm , 30-35 μm i 50-60 μm dužine dijagonale, odnosno, zavisno od uzorka. Dubina otisaka je oko 1/7 dijagonale otisaka, t.j. 1-1,4 μm , 4,3-5 μm i 7,1-8,5 μm za tri merenja sile. Korišćeno je 30-ak rampi za opterećenje, uz vreme držanja od 10 s na maksimalnom opterećenju.

Heterogena mikrostruktura je karakterisana pomoću difrakcije povratnog rasipanja elektrona (EBSD). EBSD analiza heterogenih metala šava u uzorku CV.2 (lokacija A2) je izvedena pre merenja tvrdoće na obeleženim području. Pokretni skenirajući elektronski mikroskop Zeiss Ultra 55 opremljen Nordlys F + kamerom i Kanal 5 softverom-Oxford Instruments je korišćen za EBSD analize. Analize EBSD su izvedene sa korakom od 0,2 μm pri uvećanju 1000 \times (područje 373 \times 280 μm). Napon ubrzanja je 20 kV sa graničnim kriterijumom dezorijentacije granica zrna od 10 $^\circ$. Stopa indeksiranja EBSD mapa bio je oko 90%, a podaci o EBSD su naknadno obrađeni pomoću čiste putanje najbliže oblasti.

size of $0.2\ \mu\text{m}$ at a magnification of $1000\times$ (area $373\times 280\ \mu\text{m}$). The acceleration voltage was $20\ \text{kV}$ and the grain boundary misorientation criteria of 10° were used. Indexing rate of the EBSD maps was approximately 90% and the EBSD data was post-processed using a nearest neighbour clean-up routine. The grain boundary maps from EBSD analysis were overlaid on optical micrographs and digital image processing applied in order to de-skew the distortions caused by stage drift during acquisition [35]. For optical micrographs, the samples were etched with a 2% Nital solution. Digital image processing was carried out to create grain boundary maps from the optical micrographs for base metal and homogeneous weld metal; see [31] for more details.

Mape granica zrna iz analize EBSD su preklopljena sa optičkim mikrografijama i primenjena je digitalna obrada slike kako bi se ispravila distorzija uzrokovana u fazi zanošenja tokom akvizicije [35]. Za optičke mikrografije, uzorci su nagriženi sa 2% nitalom. Digitalna obrada slike je izvršena radi stvaranja mape granice zrna iz optičkog mikrografova za osnovni materijal i homogenih metal šava; vidi [31] za više detalja.

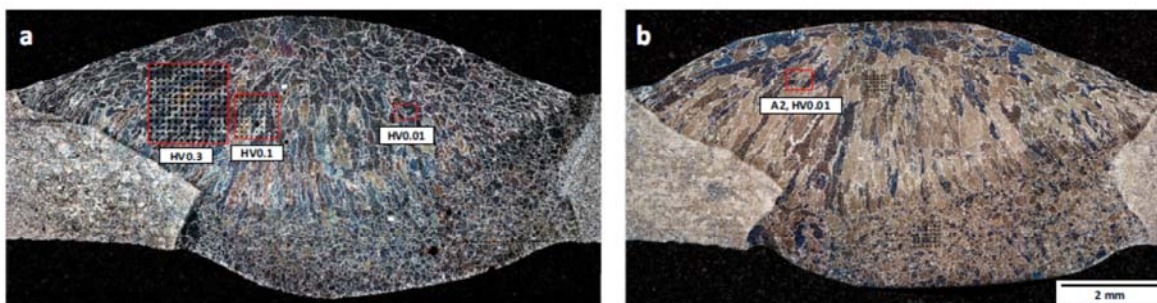


Fig. 5 Two macro sections of the arc welded joint CV.2 showing the hardness measurement locations of the heterogeneous weld metal presented in a Fig. 11 and b Fig. 12

Sl. 5. Dva makropreseka elektro-lučno zavarenog spoja CV.2 koji pokazuju lokacije merenja tvrdoće heterogenog metala šava prisutnog na sl. 11 i 12

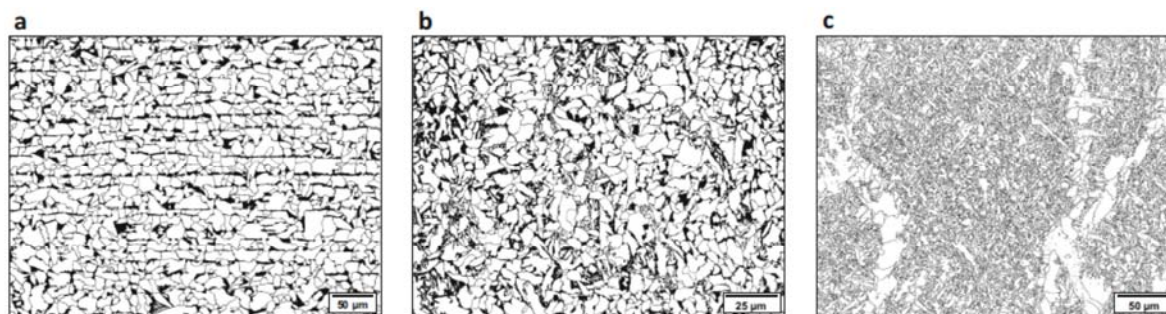


Fig. 6 The grain boundary maps used for grain size analysis of a base metal, b homogeneous weld metal and c heterogeneous weld metal

Sl. 6. Mape granica zrna koje su korišćene za analizu a) osnovnog materijala, b) homogenog metala šava i c) heterogenog metala šava

4 Results

4.1 Microstructure and grain size

The microstructures of the three specimens are shown in Fig. 6. The measured average grain sizes (d , d_v) of the single micrographs and the dimensions of the averaging line probes are presented in Table 3. The line probes are 10-pixel wide and thus the magnification of the micrograph affects the width of the probe. The relative grain

4. Rezultati

4.1. Mikrostruktura i veličina zrna

Mikrostrukture tri uzorka prikazani su na sl. 6. Izmerene prosečne veličine zrna (d , d_v) pojedinačne mikrografije i dimenzije prosečnih linijskih sondi su prikazane u tabeli 3. Linijske sonde su širine 10-piksela, a time i uvećanja mikrografije utiču na širinu sonde. Relativne

size dispersion values for the three specimens are defined based on [23]:

$$\frac{\Delta d}{d} = \frac{d_{max} - d_{min}}{d} = \frac{d_{99\%} - d_{1\%}}{d}, \quad (4)$$

where the maximum and minimum grain sizes are taken as 99 and 1 % probability level grain sizes, respectively. This value characterises the grain size dispersion on a macroscopic scale for the entire micrograph, see Ref [23] for further details. The local grain size variation found in base metal as well as homogeneous and heterogeneous weld metals are compared in Fig. 7. Base metal and homogeneous weld metal have quite homogeneous grain size as is indicated by the relative grain size dispersion. The local variation of grain size is not significant and moreover the local variation is homogeneous throughout the microstructure. On the contrary, local variation of grain size is significant for the heterogeneous weld metal. The coarse-grained areas have inconsistent spacing as shown in Fig. 7c, and thus one grain boundary map of size $345 \times 266 \mu\text{m}$ does not fully represent the length scale at which the coarse and fine-grained areas alternate.

vrednosti disperzija veličine zrna, za tri uzorka su definisane na osnovu [23]:

gde su maksimalne i minimalne veličine zrna uzete kao 99% i 1% veličine nivoa verovatnoće zrna. Ova vrednost karakteriše veličine disperzije zrna na makroskopskoj skali za celu mikrografiju, pogledajte Ref [23] za više detalja. Lokalna varijacija veličine zrna nađena je u osnovnom materijalu, kao i u homogenim i heterogenim metalima šava u poređenju sa sl. 7. Osnovni materijal i homogeni metal šava imaju prilično homogenu veličinu zrna kao što je indikovano relativnom disperzijom veličine zrna. Lokalne varijacije veličine zrna nisu značajne i štaviše lokalna varijacija je homogena kroz mikrostrukturu. Nasuprot tome, lokalne varijacije veličine zrna su značajne za heterogene šavove. Područja krupnog zrna imaju nekonzistentan razmak kao što je prikazano na slici. 7c, i na taj način mapa granice jednog zrna veličine $345 \times 266 \mu\text{m}$ ne predstavlja dužinu skale u potpunosti, na kojoj postoje područja grubog i sitnog zrna.

	Grain size			Line probes dimensions			Grain per line length	
	d (μm)	$\Delta d/d$ (-)	d_v (μm)	Line width (μm)	Horizontal (μm)	Vertical (μm)	Horizontal (-)	Vertical (-)
Base metal	10,18	3,16	15,43	1,84	532	385	35	25
Homogeneous weld	3,47	3,60	5,94	0,74	213	154	36	26
Heterogeneous weld	2,21	5,38	5,01	0,98	321	241	64	48

Grain per line length is defined as line length divided by the volume-weighted average grain size

Table 3. Measured average grain sizes for the three microstructures presented in Fig. 6 and dimensions of the line probes used for grain size averaging

	Veličina zrna			Dimenzije linijske sonde			Zrna po dužini linije	
	d (μm)	$\Delta d/d$ (-)	d_v (μm)	širina linije (μm)	horizontalno (μm)	vertikalno (μm)	horizontalno (-)	vertikalno (-)
osnovni materijal	10,18	3,16	15,43	1,84	532	385	35	25
homogeni šav	3,47	3,60	5,94	0,74	213	154	36	26
heterogeni šav	2,21	5,38	5,01	0,98	321	241	64	48

Zrna po dužini linije se definiše kao dužina linije podeljena sa zapreminski zasnovanom prosečnom veličinom zrna

Tabela 3. Izmerene prosečne veličine zrna za tri mikrostrukture prikazane na sl.6 i dimenzije linijskih sondi za određivanje prosečne veličine zrna

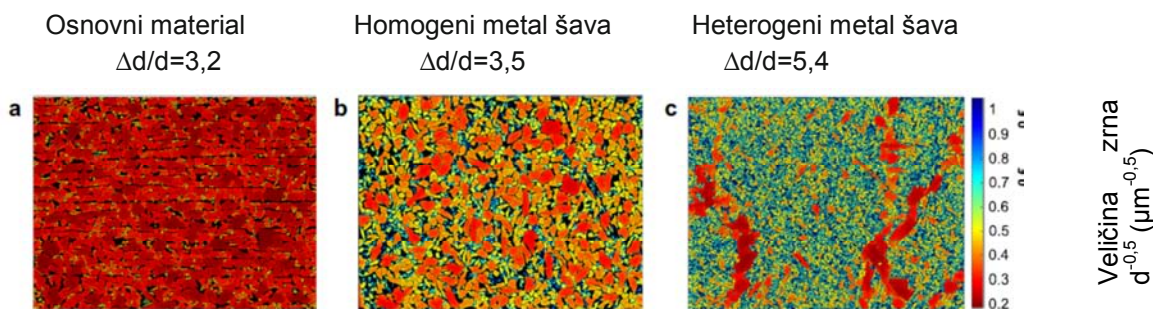


Fig. 7 Comparison of local grain size variation for S355 base metal, homogeneous and heterogeneous weld metals. The colour contours range between 0.18 and $1.05 \mu\text{m}^{-0.5}$, representing the largest 99 % and smallest 1 % probability level grain sizes for the three specimens

Sl. 7. Poređenje varijacije veličine lokalnih zrna za S355 osnovni materijal, homogeni i heterogeni metal šava. Konture boja u rasponu od $0,18$ i $1,05 \mu\text{m}^{-0.5}$, što predstavlja najveću 99%, i najmanju 1% verovatnoću veličine nivo zrna, za tri uzoraka

4.2 Characterisation of the local grain size variation

The local grain size variation of base metal, homogeneous weld metal and heterogeneous weld metal is shown in Figs. 8, 9, and 10, correspondingly. The dimensions of the line probes used for the calculation of moving averages are presented in Table 3. It can be seen that the grain size of the base metal (Fig. 8) is very uniform when the mechanical properties are considered on grain scale according to the Hall–Petch relationship ($d^{-0.5}$). Variation around the volume-weighted average grain size (d_v) is minor for the moving average of the mean grain size. In terms of grain size, it is difficult to find strong or weak locations in the microstructure as the smallest and largest grains are within a narrow band of approximately $0.2\text{--}0.5 \mu\text{m}^{-0.5}$. For homogeneous weld metal (Fig. 9), the variation of grain size is very similar to base metal, with little variation around the volumeweighted average grain size. Relatively, the minimum and maximum are further away from the mean curve, which is related to the broader grain size dispersion compared to base metal. This is visible as an increased amount of fine grains (acicular ferrite, AF) in between the coarse grains (primary ferrite, PF). For heterogeneous weld metal (Fig. 10), the location of coarse grains can be determined both visually and using the horizontal moving average of grain size. The areas with coarse grains are primary ferrite while fine-grained areas consist mostly of acicular ferrite. Furthermore, there is also noticeable grain size variation within acicular ferrite. Of the three specimens, the difference between minimum and maximum moving averages is largest for the heterogeneous weld metal in the area that consists primarily of acicular ferrite (X-coordinate $100\text{--}200 \mu\text{m}$).

4.2 Karakterizacija lokalne promene veličine zrna

Varijacija lokalne veličine zrna osnovnog materijala, homogenog metala šava i heterogenog metala šava je prikazana na slikama 8, 9, i 10. Dimenzije linijskih sondi korišćenih za obračun pokretnih proseka prikazani su u tabeli 3. Može se videti da je veličina zrna osnovnog materijala (Sl. 8) vrlo ujednačena, kada se u obzir mehanička svojstva na skali zrna po Hall-Petch odnosa ($d^{-0.5}$). Varijacija oko proseka zapreminski procenjene veličine zrna (d_v) je manja za pokretni prosek veličine srednjeg zrna. U pogledu veličine zrna, teško je naći jake ili slabe lokacije u mikrostrukturi jer su najmanja i najveća zrna u uskom opsegu od oko $0.2\text{--}0.5 \mu\text{m}^{-0.5}$. Za homogeni metal šava (Sl. 9), varijacija veličine zrna je vrlo slična osnovnom materijalu, s malo varijacija oko zapreminski procenjene prosečne veličine zrna. Relativno, minimum i maksimum su daleko od središnje krive, koja se odnosi na širu disperziju veličine zrna u poređenju sa osnovnim materijalom. To je vidljivo kao povećani iznos finih zrna (acikularni ferit, AF) između grubih zrna (primarni ferit, PF). Za heterogeni metal šava (Sl. 10), lokacija grubih zrna može se odrediti i vizuelno i pomoću horizontalno pomerljivih proseka veličine zrna. Oblasti sa grubim zrnima su primarni ferit dok se područja finog zrna sastoje uglavnom od acikularnog ferita. Osim toga, primetna je i varijacija veličine zrna unutar acikularnog ferita. Od tri uzoraka, razlika između minimalnog i maksimalnog pokretnog proseka je najveći za heterogeni šav u području koje se sastoji uglavnom od acikularnog ferita (X-koordinata $100\text{--}200 \mu\text{m}$).

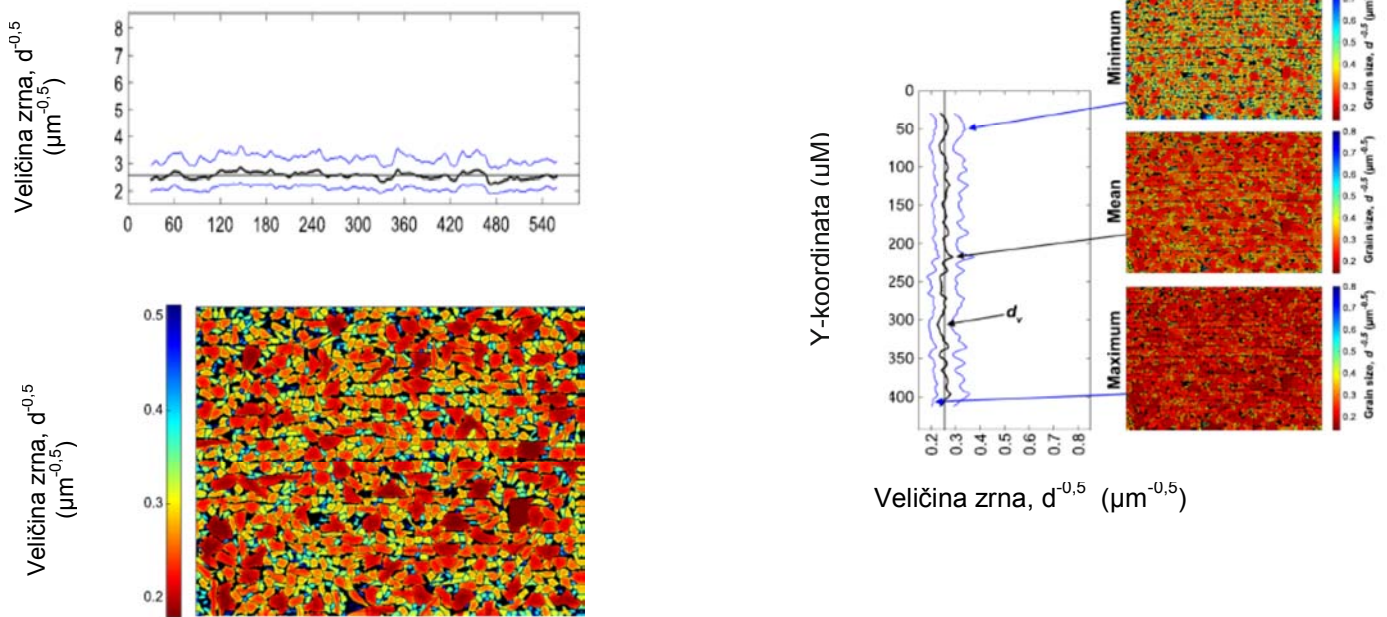


Fig. 8 Grain size plotted as a function of the Hall–Petch grain size parameter ($d^{-0.5}$) for the base metal (S355). The colour contour ranges from 99 to 1% probability level grain size for the main figure. The colour contour range is extended for the side figures to cover the 1 and 99 % probability level grain sizes of the minimum and maximum cases

SI. 8. Veličine zrna ucrtane kao funkcija parametra veličine zrna Hall-Petch ($d^{-0,5}$) za osnovni materijal (S355). Konture boja kreću se od 99% do 1% nivoa verovatnoće veličine zrna za glavnu sliku. Raspon boja kontura je proširen sa strane sa veličinama za 1% i 99% nivo verovatnoće veličine zrna za minimalne i maksimalne slučajeve.

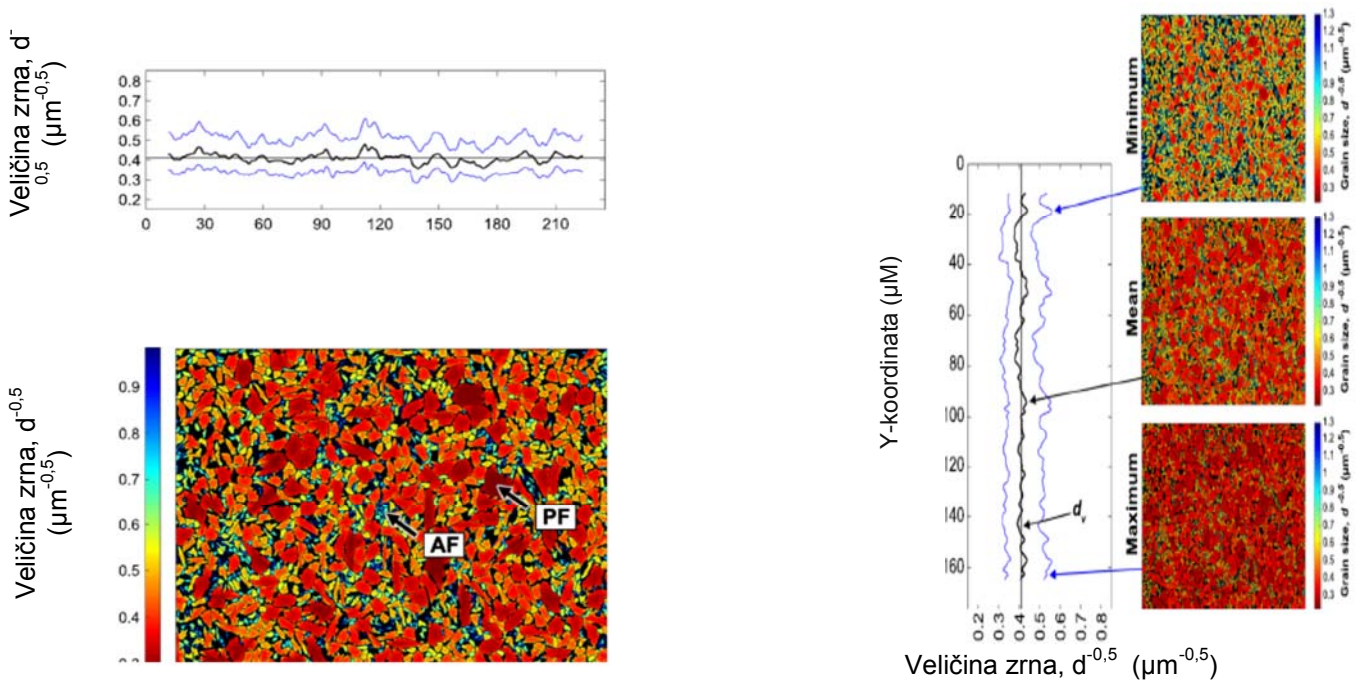


Fig. 9 Grain size plotted as a function of the Hall–Petch grain size parameter ($d^{-0.5}$) for the homogeneous weld metal. The colour contour ranges from 99 to 1% probability level grain size for the main figure. The colour contour range is extended for the side figures to cover the 1 and 99 % probability level grain sizes of the minimum and maximum cases

SI. 9. Veličina zrna ucrtana kao funkcija parametra veličine zrna Hall-Petch ($d^{-0,5}$) za homogeni šav. Konture boja kreću se od 99% do 1% nivoa verovatnoće veličine zrna za glavnu sliku. Raspon boja kontura je proširen sa strane sa veličinama za 1% i 99% nivo verovatnoće veličine zrna za minimalne i maksimalne slučajeve

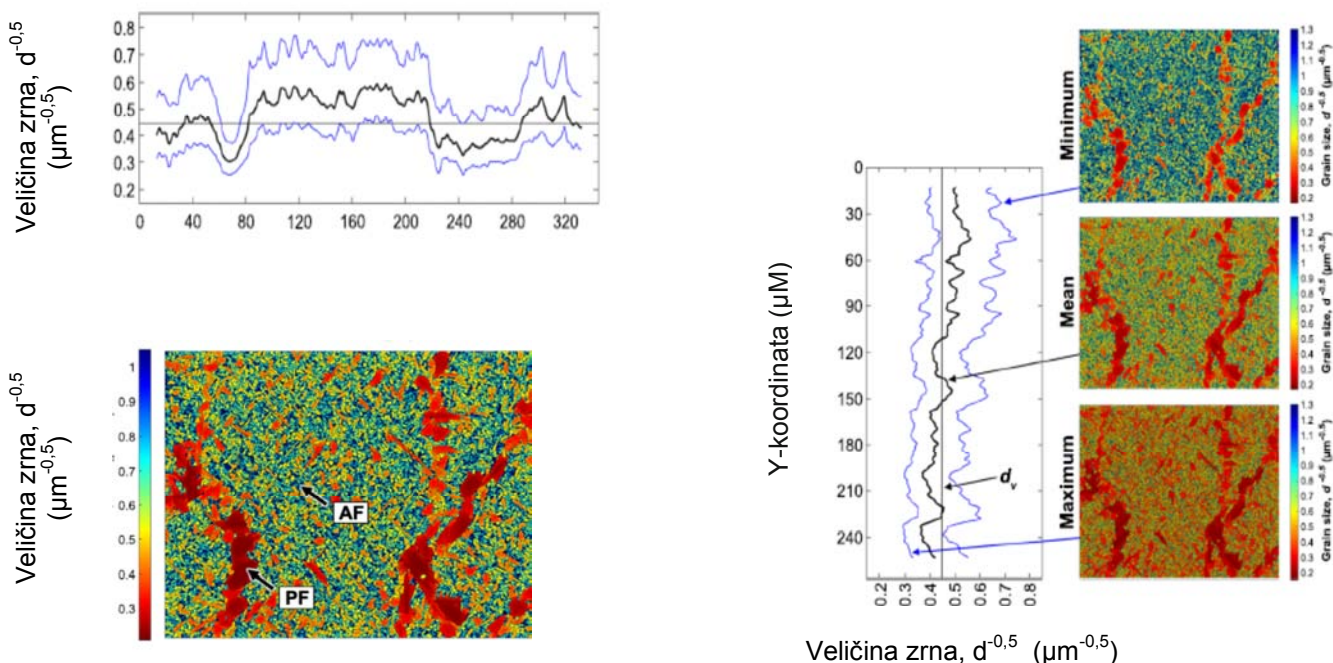


Fig. 10 Grain size plotted as a function of the Hall–Petch grain size parameter ($d^{-0.5}$) for the heterogeneous weld metal. The colour contour ranges from 99 to 1% probability level grain size for the main figure. The colour contour range is extended for the side figures to cover the 1 and 99 % probability level grain sizes of the minimum and maximum cases

Sl. 10. Veličina zrna ucrтана kao funkcija parametra veličine zrna Hall-Petch ($d^{-0,5}$) za heterogeni šav. Konture boja kreću se od 99% do 1% nivoa verovatnoće veličine zrna za glavnu sliku. Raspon boja kontura je proširen sa strane sa veličinama za 1% i 99% nivo verovatnoće veličine zrna za minimalne i maksimalne slučajeve

4.3 Comparison of hardness variation in S355 base metal and weld metal

The variation in grain size indicates that the mechanical properties might also vary significantly within the heterogeneous microstructure. The local variation in hardness measured using test forces HV0.01, HV0.1 and HV0.3 is shown in Fig. 11. The diagonal lengths of the indentations are approximately 7–10 μm , 30–35 μm and 50–60 μm , respectively. For clarity, the grain size comparison presented in Fig. 7 is from the same specimens but not at the exact location of the hardness measurements. Hardness is presented as an interpolated colour contour, and thus, it should be noted that the values in between the indentations do not represent real hardness values.

For all specimens, it is observed that the mean hardness value increases with a decrease in indentation size. At the same time, the maximum hardness values increase significantly while minimum values remain approximately the same. Using the smallest test force of HV0.01, the difference between lowest and highest measured hardness values is significant, up to 0.9 times the average value.

4.3 Upoređenje promene tvrdoće u osnovnom materijalu S355 i metalu šava

Varijacija u veličini zrna pokazuje da mehanička svojstva mogu značajno da variraju unutar heterogene mikrostrukture. Lokalne varijacije izmerene tvrdoće korišćenjem sila HV0.01, HV0.1 i HV 0.3 prikazane su na slici 11. Dijagonale dužine otisaka su oko 7-10 μm , 30-35 μm i 50-60 μm . Zbog jasnoće, odnos veličine zrna prikazan na Sl. 7 je iz istih uzoraka, ali ne na tačnim lokacijama merenja tvrdoće. Tvrdoća je predstavljena kao interpolisana kontura u boji, i na taj način, treba napomenuti da vrednosti između otisaka ne predstavljaju prave vrednosti tvrdoće.

Za sve uzorke, uočeno je povećanje srednje vrednosti tvrdoće sa smanjenjem veličine otiska. U isto vreme, maksimalne vrednosti tvrdoće značajno rastu, a minimalne vrednosti ostaju približno iste. Koristeći najmanju ispitnu silu HV0.01, razlika između najniže i najviše izmerene vrednosti tvrdoće je značajna, do 0,9 puta od prosečne vrednosti.

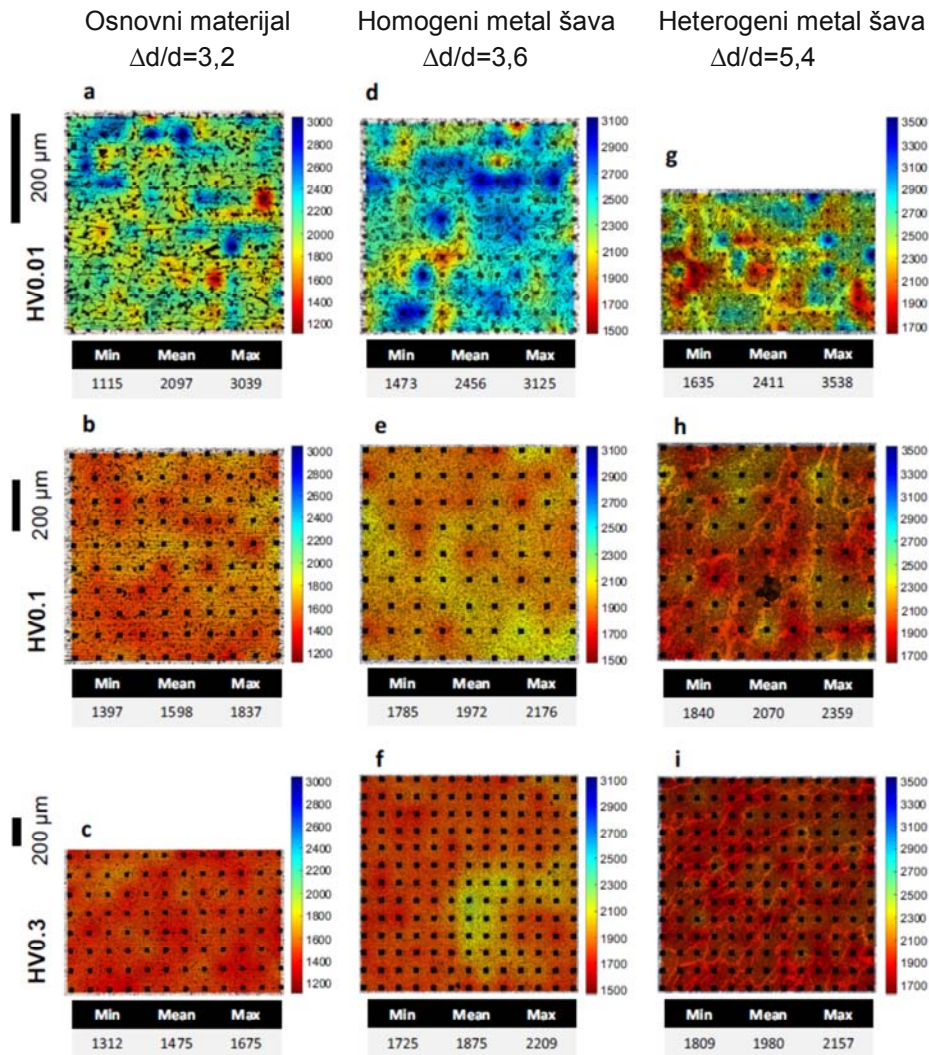


Fig. 11 Comparison of local hardness variation (HM) using three different indentation loads for the three specimens. The colour scales range between HV0.01 minimum and maximum for each specimen

Sl. 11 Poređenje varijacije lokalnih tvrdoća (HM) pomoću tri različita opterećenja za tri uzorka. Skale boja u rasponu od HV0.01 minimum i maksimum za svaki uzorak

This can be related to the placement of the small indentations in the microstructure, hitting e.g. entirely in soft ferrite grain interiors or hard pearlite. While base metal and homogeneous weld metal generally show smooth transitions between low and high hardness areas, the heterogeneous weld metal shows much higher local variation. This is the case particularly for the HV0.01 measurement force that produces small, 7–10 μm indentations. At higher test forces of HV0.1 and HV0.3, base metal and homogeneous weld metal show variation in hardness even though the grain size is very uniform in the structure. Likewise, with HV0.3 indentations, the local variation in hardness cannot be captured for the heterogeneous weld metal since the indentations are larger than the coarse-grained areas. Thus, it is challenging to choose indentation parameters; indentation size in relation to grain size and at the same time the spacing of indentations

To se može odnositi na postavljanje malih otisaka u mikrostrukтури, pogađanje npr. potpuno mekih feritnih zrna ili tvrdog perlita. Dok osnovni materijal i homogeni metal šava generalno pokazuju blage prelaze između područja niske i visoke tvrdoće, heterogeni šav pokazuje mnogo veće lokalne varijacije. Ovo je posebno slučaj za HV0.01 silu merenja koja proizvodi male, 7-10 μm otiske. Pri većim ispitnim silama HV0.1 i HV0.3, osnovni materijal i homogeni metal šava pokazuju varijacije u tvrdoći, iako je veličina vrlo uniformna u strukturi. Isto tako, s HV0.3 otiscima, lokalne varijacije tvrdoće ne mogu biti vezane za heterogeni šav jer su otisci veći nego u području krupnog zrna. Dakle, to je izazov da se izaberu parametri otisaka; veličina otiska u odnosu na veličinu zrna i istovremeno razmak između otisaka utiču na podatke prikupljene iz prethodno određenog

affects the data gathered from a predetermined area. The transition and relations between different size indentations, as well as the relation to tensile properties require further study.

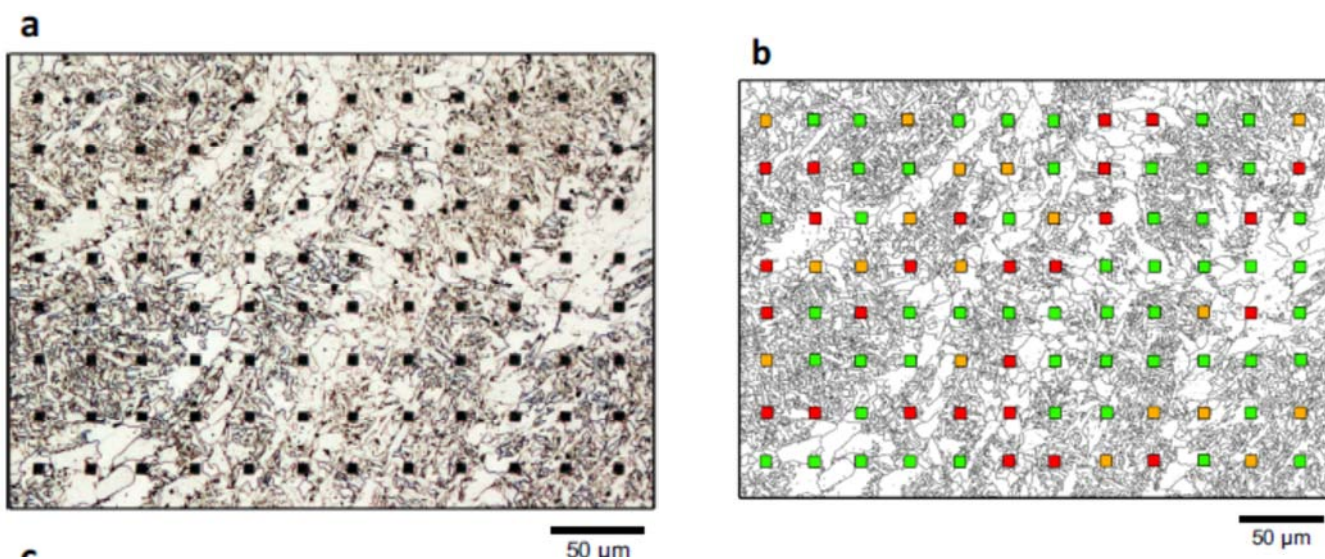
4.4 Correlation between grain size and hardness

To investigate the local grain size variation, additional hardness measurements were carried out for the heterogeneous weld metal. Prior to hardness measurements, an EBSD analysis was carried out at location A2 of the weld (see Fig. 5) that was pre-marked with hardness indentations. After hardness measurements, the specimen surface was etched, which enables overlaying of the EBSD maps on the microstructure and identifying the location of hardness indentations. The hardness data and grain size contour for the studied heterogeneous weld metal are shown in Fig. 12. The figure contains (a) an optical micrograph of the hardness measurements, (b) visual estimate of correlation between hardness and local microstructure and (c) hardness in discrete form for individual indentations overlaid on the grain size contour. The visual estimate in (b) is divided into three categories: (1) green, grain size under the indentation correlates with hardness within approximately ± 100 HM (52/96 samples, 54 %); (2) orange, hardness correlates with grain size when the microstructure surrounding the indentation is considered (18/96, 19 %) and (3) red, hardness and local grain size show no correlation (26/96, 27 %). Reader is referred to Appendix 2 for the hardness values and a figure that shows the grain size under and around each indentation.

područja. Prenos i odnos između različitih veličina otisaka, kao i odnos prema zateznim svojstvima zahtevaju dalje proučavanje.

4.4. Korelacija između veličine zrna i tvrdoće

Da bi istražili lokalne varijacije veličine zrna, izvršena su dodatna merenja tvrdoće za heterogeni šav. Pre merenja tvrdoće, analiza EBSD izvršena je na lokaciji A2 šava (vidi sl. 5) koji je bio prethodno označen otiscima merenja tvrdoće. Nakon merenja tvrdoće, površina uzorka je nagrižena, što omogućava prevlačenje EBSD mape na mikrostrukturu i identifikaciju lokacija otisaka tvrdoće. Podaci o tvrdoći i kontura veličine zrna za istraživani heterogeni šav prikazani su na slici. 12. Slika sadrži (a) optičku mikrografiju merenja tvrdoće, (b) vizuelnu procenu korelacije tvrdoće i lokalnih mikrostruktura i (c) tvrdoća u diskretnom obliku za pojedinačne otiske preklapljeno konturom veličine zrna. Vizuelna procena u (b) je podeljena u tri kategorije: (1) zelena, veličina zrna pod otiscima u korelaciji sa tvrdoćom od približno ± 100 HM (52/96 uzoraka, 54%); (2) narandžasta, tvrdoća u korelaciji sa veličinom zrna kada se razmatra mikrostruktura oko otisaka (18/96, 19%) i (3) crvena, tvrdoća i lokalne veličine zrna ne pokazuju korelaciju (26/96, 27%). Čitalac se upućuje na Dodatak 2 za tvrdoće i sliku koja prikazuje veličine zrna ispod i oko svakog otiska.



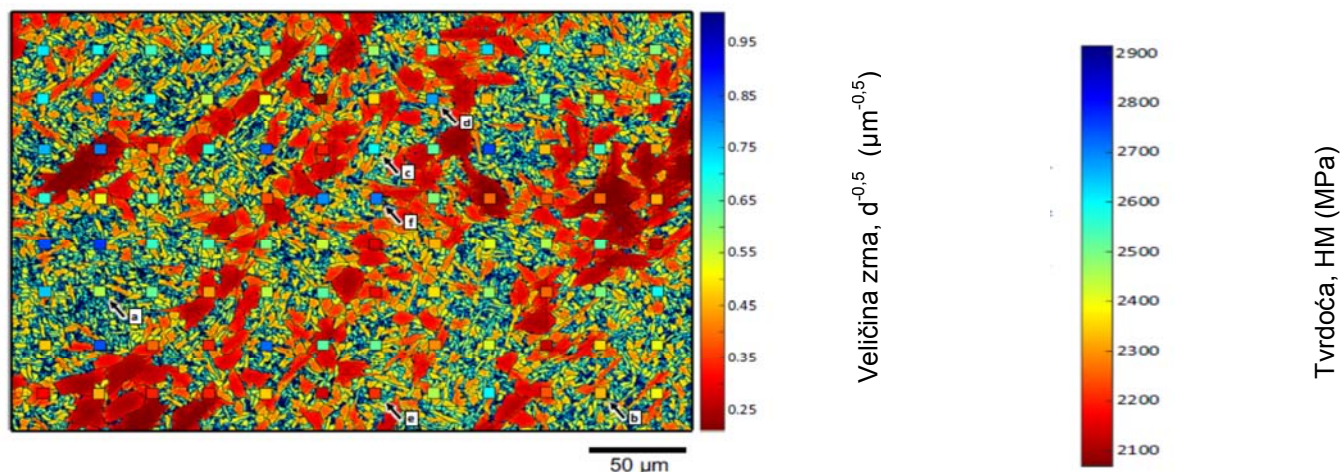


Fig. 12 a Optical micrograph of the hardness measurement area for the heterogeneous weld metal area A2, **b** grain boundary map and visual estimation of the correlation between local grain size and hardness; see text for the explanation and **c** the hardness value for each indentation overlaid on the grain size contour, ranging from 99 to 1% probability level grain size

Sl. 12. a) Optička mikrografija površine merenja tvrdoće na površini A2 heterogenog metala šava, b) mapa granica zrna i vizuelno određivanje korelacije između lokalne veličine zrna i tvrdoće; videti tekst za objašnjenje i c) vrednost tvrdoće za svaki otisak koji se preklapa sa konturom veličine zrna, u opsegu od 99% do 1% nivoa verovatnoće veličine zrna

In general, the low hardness areas correspond with the coarse grains and high hardness with the fine-grained areas. A mixture of different grain sizes under the indentation is found to result in a measured hardness value that corresponds approximately with the average grain size of the area according to the rule of mixtures; see Fig. 13a. When fine grains are surrounded by coarse grains, hardness is found to decrease, and in the opposite case, to increase; see Fig. 13b, c, correspondingly. Placement of the indentation tip in a small cluster of fine grains is found to increase the hardness value, even though the microstructure under and around the indentation would otherwise consist of coarse grains; see Fig. 13d. In some cases, low hardness is measured in fine grains and high hardness in coarse grains; see Fig. 13 e, f, correspondingly. Further numerical analysis of the microstructure at each indentation is required before correlations between local microstructure and hardness can be formulated.

5. Discussion

The local grain size and hardness variation of ferritic base metal and two weld metals were studied. The point-sampled intercept length method was extended for the characterisation of local grain size variation. The local gradient of grain size variation and its dependency on measurement direction were considered. Base metal and homogeneous weld metal did not have significant local grain size variation, while the heterogeneous weld metal had distinct areas of coarse and fine grains. The coarse-grained areas are associated with primary ferrite and the fine-grained areas with acicular ferrite. Hardness was measured to

U principu, područja niske tvrdoće odgovaraju grubom zrnju a visokoj tvrdoći, područja sa finim zrnjom. Mešavina različitih veličina zrna ispod otiska je dovela do izmerene vrednosti tvrdoće koja odgovara otprilike prosečnoj veličini zrna područja u skladu sa pravilima mešavine; vidi sliku. 13a. Kada su fina zrna okružena grubim zrnima, tvrdoća se smanjuje, a u suprotnom slučaju, se povećava; vidi sliku 13b. Postavljanje vrha otiska u malom klasteru finog zrna, povećava se vrednost tvrdoće, iako se mikrostruktura ispod i oko otiska inače sastoji od grubog zrna; vidi sliku 13d. U nekim slučajevima, niska tvrdoća je izmerena na finim zrnima a visoka tvrdoća kod grubih zrna; vidi sliku 13e, f. Dalja numerička analiza mikrostrukture na svakom otisku je potrebna pre nego što se korelacija između lokalnih mikrostrukture i tvrdoće može formulirati.

5. Diskusija

Varijacije lokalne veličine zrna i tvrdoće feritnih osnovnih materijala i dva metala šava su proučavane. Metoda tačkastog uzorkovanja dužine otisaka je produžena na karakterizaciju varijacije lokalne veličine zrna. Razmatrani su lokalni gradijent varijacije veličine zrna i njegove zavisnosti od smera merenja. Osnovni materijali i homogeni metal šava nisu pokazali značajne varijacije lokalne veličine zrna, dok heterogeni šav ima različita područja grubih i finih zrna. Područja krupnog zrna su povezana sa primarnim feritom i sitnozrnim područjima sa acikularnim feritom.

Tvrdoća je merena radi istraživanja uticaja varijacije lokalne veličine zrna na mehanička svojstva. EBSD analiza veličine zrna se obično izvodi pomoću identifikacije zrna i određivanja veličine zrna sa

investigate the influence of local grain size variation on mechanical properties. EBSD grain size analysis is typically carried out using the grain identification and determination of grain size from its surface area, often taken as the diameter of a circle with an equivalent surface area [12, 36]. For homogeneous equiaxed microstructures, this assumption is justified, and values determined by circle equivalent diameter (d_{ceq}) and linear intercept are comparable within 10 % of each other [15]. The use of circle equivalent diameter has limitations when applied to heterogeneous weld metal microstructures. Welds can have microstructures where definition of individual grains is ambiguous due to discontinuities in the grain boundaries, and thus clusters of multiple grains can be detected as a single grain. This has been demonstrated for stainless steel pipe welds by Saukkonen et al. [37], also showing the robustness of the linear intercept method to EBSD indexing errors and the consequent grain detection. Furthermore, the circle equivalent diameter is not well suited for high aspect ratio grains by itself, and more information about the shape of the grain is required [38]. For welds, the high aspect ratio of grains, as well as morphological anisotropy, make the assumption of circular geometry invalid. Thus, the volume-weighted linear intercept method should be preferred for grain size measurement of heterogeneous weld microstructures with complex grain morphologies. To that end, the methodology presented here is able to consider the aspect ratio of grains through the four measurement directions. Although limited to four measurement directions, it seems sufficient for the characterization of weld metal microstructures.

svoje površine, često se uzima kao prečnik kruga sa ekvivalentnim površinama [12, 36]. Za homogene istoosne mikrostrukture, ova pretpostavka je opravdana, i vrednosti određuje krug ekvivalentnog prečnika (d_{ceq}) i linearno preklapanje je uporedivo do 10% jedno sa drugim [15]. Upotreba kruga ekvivalentnog prečnika ima ograničenja kada se primjenjuje na mikrostrukturama heterogenih šavova.

Šavovi mogu imati mikrostrukturu gde je dvosmisleno definisano pojedino zrno zbog diskontinuiteta u granicama zrna tako da klaster više zrna može biti prepoznat kao zrno. To je demonstrirano na zavarenim spojevima čeličnih cevi po Saukkonen i dr. [37], takođe pokazuje robusnost metode linearnog preklapanja na EBSD indeksiranje grešaka i posledično otkrivanje zrna. Osim toga, krug ekvivalentnog prečnika nije dobro prilagođen za visoki aspekt zrna po sebi, a potrebno je i više informacija o obliku zrna [38]. Za šavove, visok odnos aspekata zrna, kao i morfološka anizotropija, čine pretpostavku kružne geometrije nevažecom. Dakle, zapreminski procenjena linearna metoda ima prednost kod merenja veličine zrna mikrostrukture heterogenih šavova složene morfologije zrna. U tom smislu, ovde predstavljena metodologija je u stanju uzeti u obzir, odnos aspekata zrna za četiri smera merenja. Iako je ograničen na četiri smera merenja, to je i dovoljno za karakterizaciju metala mikrostruktura šava.

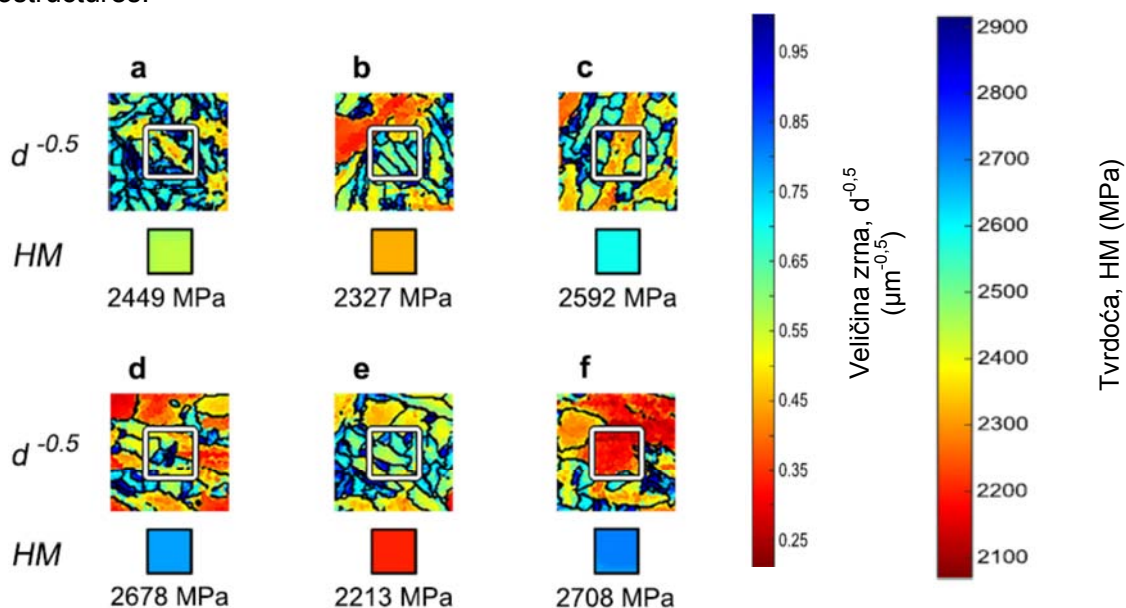


Fig. 13 Expanded view of grain size and hardness at indentations a–f indicated in Fig. 12c

Sl. 13. Prošireni izgled veličine zrna i tvrdoće po otiscima a–f označenim na sl. 12 c

It is also not sensitive to small discontinuities in the grain boundaries that are observed in welded [39, 40] and deformed [41] steel microstructures. For a physically based definition, the grain size measurement direction should be parallel with the direction of the slip plane in each grain, requiring the utilisation of orientation information in grain size measurement. As the present approach is based on measurement of 2D sections, the morphological anisotropy of the grains is not considered.

Grain size variation was found to be significant within acicular ferrite in the heterogeneous weld metal, having the biggest relative difference between the minimum and maximum grain size curves in Fig. 10. The variation is related to the high aspect ratio of the grains, resulting in a significant difference between the shortest and longest grain size measurement directions.

Local variation of grain size is visually significant within acicular ferrite, as shown in Figs. 10 and 12c, ranging approximately between 1 and 5 μm even though not revealed by the moving average line probe. The line probes are influenced by the number of grains falling under the line, and thus, the true variation will average out with a large number of grains. This is the case for acicular ferrite in the heterogeneous weld metal, and further research is required to define methods better suited for quantifying the local grain size variation numerically.

Even though the base metal and homogeneous weld metal are uniform in grain size, hardness measurements revealed low and high hardness regions using HV0.1 and HV0.3 test forces; see Fig. 11b, c, e and f. Visually, the grain size is uniform through the entire microstructure, and thus, it seems that factors other than grain size contributed to the observed differences. Hardness measurements using HV0.01 test force revealed that in the heterogeneous weld metal, the low hardness values are usually associated with coarse grains and high hardness values with fine grains, as is expected by the Hall–Petch relationship [8, 9]; see Fig. 12c. Despite the visual estimate of 54 % of hardness measurements corresponding with the local grain size (Fig. 12b), variation is observed between regions of similar grain size. This can be caused by differences in grain orientation [42, 43] and dislocation slip transmission between grains [44, 45]. The plastic zone from a hardness indentation is hemispheric, extending 1.0–1.9 times the contact radius with the highest plastic strain (>20 %) located directly underneath the indenter contact region [46]. Therefore, the microstructure of the entire plastic zone will influence the hardness

Takođe nije osetljiv na male diskontinuitete u granicama zrna koji su primećeni u zavarenim [39, 40] i deformisanim [41] mikrostrukturama čelika. Za fizički zasnovanu definiciju, pravac merenja veličine zrna trebalo bi da bude paralelan sa pravcem ravni klizanja u svakom zrnju, zahteva korišćenje informacija o orijentaciji merenja veličine zrna.

Kao što se sadašnji pristup zasniva na merenju 2D preseka, morfološka anizotropija zrna se ne razmatra.

Utvrđeno je da je varijacija veličine zrna značajna kod acikularnog ferita u heterogenom metalu šava, jer ima najveću relativnu razliku između minimalne i maksimalne krive veličine zrna na Sl. 10. Varijacija se odnosi na visoki odnos aspekata zrna, što je dovelo do značajne razlike između najkraćeg i najdužeg pravca merenja veličine zrna.

Lokalne varijacije veličine zrna su vizuelno značajne kod acikularnog ferita, kao što je prikazano na slikama. 10 i 12c, u rasponu između 1 i 5 μm , iako nije otkriven pokretni prosek linijske sonde. Linijske sonde su pod uticajem broja zrna koja padaju ispod linija, i na taj način, stvarna varijacija biće u proseku sa velikim brojem zrna. Ovo je slučaj za acikularni ferit u heterogenim metalu šava, i dalje istraživanje je potrebno za definisanje pogodnijih metoda za brojčano kvantifikovanje varijacije lokalne veličine zrna.

Iako su veličine zrna u osnovnom materijalu i homogenom metalu šava uniformne, merenjem su utvrđene regije niske i visoke vrednosti koristeći HV0.1 i HV 0.3 ispitne sile; vidi sliku. 11b, c, e i f. Vizuelno, veličina zrna je ujednačena kroz čitavu mikrostrukturu, i na taj način, čini se da i drugi faktori osim veličine zrna, doprinose uočenoj razlici.

Merenjem tvrdoće pomoću HV0.01 ispitne sile ustanovljeno je da u heterogenom metalu šava, niske tvrdoće obično povezuju s grubim zrnima a visoke vrednosti tvrdoće s finim zrna, kao što se očekuje do Hall-Petch odnosa [8, 9]; vidi sliku 12c. Uprkos vizuelnoj proceni da 54% merenja tvrdoće odgovara lokalnoj veličini zrna (sl. 12b), varijacije su zapažene između regija slične veličine zrna. Ovo može biti uzrokovano razlikama u orijentaciji zrna [42, 43] i prenosu klizanja dislokacija između zrna [44, 45]. Plastične zone iz otisaka merenja tvrdoće su hemisferične, proširujući 1,0-1,9 puta kontaktni radijus sa najvećom plastičnom deformacijom (> 20%) koje se nalaze neposredno ispod oblasti kontakta otiska [46]. Prema tome, mikrostruktura cele plastične zone će uticati na merenje tvrdoće. Ovo je vidljivo za 19% merenja

gde measurement. This is visible for the 19 % of measurements where surrounding coarse or fine grains either decreased or increased the hardness value, respectively. The limitation of observing grain size on the surface of the specimen is visible with 27 % of the measurements as the grain size is not in agreement with the measured hardness value. Furthermore, the microstructural length scale, e.g. grain size, interacts with the length scale of hardness measurements [47]. These effects become relevant with indentations small relative to the grain size, and disappear as the length scale of deformation is large relative to the microstructural heterogeneities [47]. For the heterogeneous weld metal, the coarse grains are up to 25 μm in size while the fine grains are 1–5 μm in size, and thus the plastic zone of an indentation with 7- μm diagonal and 1- μm depth can be limited to a few grains or tens of grains. Therefore, the size of the plastic zone can vary depending on grain size and should be considered in the grain size measurement. In addition to grain size characterisation, phase properties need to be considered in microstructural analysis.

Even though in case of acicular ferrite and primary ferrite the phases behave similarly in hardness measurements [23], the tensile properties and toughness can show significant differences despite similarity of grain size. Zhao [48] found that acicular ferrite ($d=4\text{--}5\ \mu\text{m}$) had lower ultimate tensile strength but higher yield strength than ultrafine-grained ferrite ($d=1\ \mu\text{m}$). The differences were attributed to carbonitride precipitation, higher dislocation density and the lath bundle size of acicular ferrite. In general, acicular ferrite is beneficial for mechanical properties and besides tensile properties it improves impact toughness and decreases the transition temperature [49, 50].

Thus, methods are sought after to increase the volume fraction of acicular ferrite in welds [49, 51]. In this study, the weld metal microstructures were examined using two dimensional analysis. Based on current analysis hardness shows good agreement (54 %) in locations where the local grain size gradient is typically small. It is expected that the gradient of grain size under the indentation has a significant effect on measured hardness values as well. It is likely that for the locations with good agreement the grain size gradient under the indentation is small or that the gradient is such that the measured hardness appears to correlate with surface grain size. For weld metals, the solidification behaviour controls the grain structure and the achieved mechanical properties [52].

se okružujuća gruba ili fina zrna ili smanjila ili povećala vrednost tvrdoće. Ograničenje u posmatranju veličine zrna na površini uzorka je to što 27% merenja veličine zrna ne odgovara izmerenim vrednostima tvrdoće.

Osim toga, mikrostrukturna dužinska skala, npr veličine zrna, u interakciji je sa dužinskom skalom merenja tvrdoće [47]. Ovi efekti postaju relevantni sa malim otiscima u odnosu na veličinu zrna, i nestaju kada je dužinska skala deformacije velika u odnosu na mikrostrukturne heterogenosti [47]. Za heterogeni šav, gruba zrna su do 25 μm veličine, a fina zrna su veličine 1-5 μm , a time i plastične zone otisaka sa dijagonalom 7- μm i dubinom 1- μm mogu biti ograničene na nekoliko zrna ili desetina zrna. Dakle, veličina plastične zone može da varira zavisno od veličine zrna i treba uzeti u obzir merenje veličine zrna. Osim karakterizacije veličine zrna, svojstva faza treba uzeti u obzir kod mikrostrukturne analize.

Iako je u slučaju acikularnog ferita i primarnog ferita, faze se ponašaju slično kod merenja tvrdoće [23], i zateznih svojstava a žilavost može pokazati značajne razlike uprkos sličnoj veličini zrna.

Zhao [48] je utvrdio da acikularni ferit ($d = 4\text{--}5\ \mu\text{m}$) ima nižu zateznu čvrstoću na zatezanje, ali veći napon tečenja od ultrafinog ferita ($d = 1\ \mu\text{m}$). Razlike su pripisane talozima karbonitrida, većoj gustini dislokacija i veličini traka acikularnog ferita. U principu, acikularni ferit je od koristi za mehanička svojstva i osim zateznih svojstava poboljšava udarnu žilavost i snižava prelaznu temperaturu [49, 50].

Dakle, metode su tražene posle da se poveća zapreminski udeo acikularnog ferita u šavu [49, 51]. U ovoj studiji, mikrostruktura metala šava je ispitana pomoću dvodimenzionalne analize. Na bazi trenutne analize tvrdoće ustanovljeno je dobro slaganje (54%) na lokacijama gde su lokalni gradijenti veličine zrna obično mali. Očekuje se da gradijent veličine zrna pod otiskom ima značajan uticaj na izmerene vrednosti tvrdoće. Verovatno da je za lokacije s dobrim slaganjem gradijenta veličina zrna pod otiskom je mala ili da je gradijent takav da je izmerena tvrdoća u korelaciji s veličinom površine zrna. Kod metala šava, ponašanje pri očvršćavanju kontroliše strukturu zrna i postignuta mehanička svojstva [52].

The competitive growth of grains, influenced by the transient thermal conditions and solidification characteristics of the weld metal, determines the morphology of the grain structure [52, 53]. In fusion welding axial, columnar and equiaxed grain morphologies can be observed depending on the thermal gradient, cooling rate and use of grain refining particles [52, 54,55]. Therefore, the appearance of the grains on one cross section may not be representative of the grain morphology [56], causing bias for the assumed relationship between surface area and volume (Eq. 3).

For example, columnar grains can appear very large on the transverse section even though the grains are quite shallow. Thus, the morphology of the grains and the anisotropy of the microstructure in the direction of the weld bead should be included in the analysis. It is expected that hardness of the heterogeneous weld metal (Fig. 12) is better predicted if the morphological anisotropy is considered. Furthermore, other obstacles to dislocation motion such as inclusions can influence the measured hardness values on a local scale. Consideration of these aspects is left for future work.

6. Conclusions

The point-sampled grain size measurement method was extended to the characterisation of local grain size variation. The Hall–Petch grain size parameter ($d^{-0.5}$) was found to give a good visual representation of grain size-dependent mechanical properties. Heterogeneous weld metal was found to have significant local variation of grain size while base metal and homogeneous weld metal were not. Furthermore, the local variation of grain size correlates with hardness measurements for a large portion of the measurements, with coarse grains generally showing low hardness and fine grains high hardness. Grain size alone was not able to explain all of the measurement results and thus future work is needed to analyse the local microstructure to determine factors other than grain size that should be included in the microstructural characterisation. In particular, the morphological anisotropy, i.e. the three dimensional shape of the grains needs to be characterized.

Acknowledgments The work has been done within the FIMECC BSA (Breakthrough Steels and Applications) programme as part of the FIMECC Breakthrough Materials Doctoral School. We gratefully acknowledge the financial support from the Finnish Funding Agency for Innovation (Tekes) and the participating companies. Funding from the Academy of Finland project BFatigue of Steel Sandwich Panels[^] (FASA) under grant agreement

Konkurentski rast zrna, pod uticajem prolaznih termičkih uticaja i karakteristike očvršćavanja metala šava, određuju morfologiju strukture zrna [52, 53]. Na liniji stapanja kod zavarivanja, stubičasta i istoosna morfologija zrna može se posmatrati u zavisnosti od termičkog gradijenta, brzine hlađenja i korišćenje rafinacije zrna česticama [52, 54,55]. Dakle, izgled zrna na nekom preseku ne može biti predstavnik morfologije zrna [56], jer uzrokuje i pretpostavke za odnos između površine i zapremine (EQ. 3).

Na primer, stubičasta zrna se mogu pojaviti kao vrlo velika na poprečnom preseku iako su zrna vrlo plitka. Stoga, morfologija zrna i anizotropija mikrostrukture u pravcu šava treba da se uključi u analizu. Očekuje se da tvrdoća heterogenog šava (sl. 12) se bolje predviđa ako se razmatra morfološka anizotropija. Osim toga, druge prepreke kretanju dislokacija kao što su uključci mogu uticati na izmerene vrednosti tvrdoće na lokalnoj skali. Razmatranje tih aspekata je ostavljeno za budući rad.

6. Zaključci

Metoda merenja veličina zrna preko tačaka je proširena na karakterizaciju varijacije lokalne veličine zrna. Utvrđeno je da Hall-Petch-ov parametar veličine zrna ($d^{-0.5}$) daje dobar vizuelni prikaz mehaničkih svojstava zavisnih od veličine zrna. Za heterogeni metal šava je utvrđeno da ima značajnu lokalnu varijaciju veličine zrna dok kod osnovnih materijala i homogenih metala šava, nije bilo. Osim toga, lokalne varijacije veličine zrna su u korelaciji sa merenjima tvrdoće za veliki deo merenja, sa grubim zrnima generalno pokazuju niske tvrdoće i sa finim zrnima, visoke tvrdoće. Samo veličinom zrna nije moguće objasniti sve rezultate merenja i na taj način, za budući rad je potrebna analiza lokalne mikrostrukture kako bi se utvrdili faktori, osim veličine zrna, koje treba uključiti u mikrostrukturnu karakterizaciju.

Posebno, morfološka anizotropija, t.j. potrebna za karakterizaciju trodimenzionog oblika zrna. Zahvalnost. Rad je deo programa FIMECC BSA (Breakthrough Steels and Applications) kao dela FIMECC Breakthrough Materials Doctoral School. Dugujemo veliku zahvalnost za finansijsku potporu Finske agencije za finansiranje inovacija (Tekes) i kompanija učesnica. Finansiranje projekta Finske akademije „Zamor čeličnih sendvič panela“ (FASA) u skladu sa sporazumom o grantu br. 261286 se zahvaljujemo s poštovanjem. Zahvaljujemo se na konstruktivnim komentarima profesora Sven

no. 261286 is gratefully appreciated. The constructive comments of Professor Sven Bossuyt from Aalto University School of Engineering are gratefully acknowledged. Tuomo Nyyssönen from Tampere University of Technology is acknowledged for providing EBSD data suitable for the preliminary development of the grain size measurement Matlab code.

Appendix 1: Vickers hardness compared to instrumented indentation hardness

Traditional hardness measurements rely on measurement of, e.g. the diagonal of the indentation after the test force has been removed. As a result, only the residual plastic deformation is considered and elastic deformation is ignored. Instrumented indentation testing (IIT) enables the evaluation of both the elastic and plastic deformation by monitoring of the test force and displacement of the indenter. In addition to hardness, other material parameters such as indentation modulus can be determined without the need for optical measurement of the indentation [34]. Due to the force-displacement data being available, several definitions can be used for defining hardness from IIT measurements, with indentation hardness (HIT) being the most commonly used parameter. However, the definition of indentation hardness [34] is the maximum force divided by the projected area, which is not the case for definition of traditional Vickers hardness. ISO 14577-1 Annex F [34] includes the correlation of HIT to Vickers hardness by converting the projected area to the surface area of contact. The correlation between the two is formulated as $HV = 0.0945 \times HIT$ based on the constant ratio of projected area to surface area and unit conversion to kg/mm^2 . It is noted that the values calculated in this manner should not be used as a substitute for Vickers hardness.

Another approach is to use Martens hardness (HM), which by definition is the same as traditional Vickers hardness. These two options are compared in Fig. 14 for the measurements of Ref. [23], although not presented there in this form. For comparability, Martens hardness is also converted to kilogrammes per millimetre squared. The ferritic weld metals (WM) have good correlation with Martens hardness and Vickers hardness below 250 HV within the $\pm 5\%$ limits. At higher values, Martens hardness values are lower than Vickers hardness, indicating that significant in-plane elastic recovery took place after the test force was removed, thus reducing the optically measured diagonals. Indentation hardness (HIT) shows higher deviation

Bossuyt-a sa Aalto University School of Engineering. Izražavamo zahvalnost g-dinu Tuomo Nyyssönen sa Tehnološkog univerziteta Tampere na ustupanju EBSD podataka pogodnih za preliminarni razvoj Matlab pravila merenja veličine zrna.

Dodatak 1: Tvrdoća po Vickersu u poređenju sa instrumentirano merenom tvrdoće otisaka

Tradicionalno merenje tvrdoće se oslanja na merenje, npr dijagonala otiska nakon što je ispitna sila uklonjena. Kao rezultat toga, samo zaostale plastične deformacije se razmatraju a elastične deformacije se zanemaruju. Instrumentovano ispitivanje otisaka (IIT) omogućava evaluaciju i elastične i plastične deformacije praćenjem ispitne sile i premeštanja otisaka. Osim tvrdoće, drugi parametri materijala kao što je modul otiska može se utvrditi bez potrebe za optičkim merenjem otisaka [34].

Zavisno od raspoloživih podataka o kretanju sila, može se koristiti nekoliko definicija za određivanje tvrdoće iz IIT merenja, sa tvrdoćom otisaka (HIT) što je najčešće korišćeni parametar. Međutim, definicija tvrdoće otisaka [34] je maksimalna sila podeljena sa projektovanom površinom, što nije slučaj za definiciju tradicionalne Vickers tvrdoće. ISO 14577-1 Aneks F [34] uključuje korelaciju HIT sa Vickers tvrdoćom pretvaranjem projektovane površine na površinu kontakta. Korelacija ova dva je formulisana kao $HV = 0.0945 \times HIT$ zasnovana na konstantnom odnosu projektovane površine na površinu a jedinica mere konverzije u kg / mm^2 . Napominje se da vrednosti izračunate na ovaj način, ne treba koristiti kao zamenu za tvrdoću po Vickersu.

Drugi pristup je korišćenje Martens tvrdoće (HM), koja je po definiciji isto kao i tradicionalna tvrdoća po Vickersu. Ove dve opcije su upoređene na sl. 14 za merenje Ref. [23], iako nije u ovom obliku ovde prikazan. Radi uporedivosti, Martens tvrdoća se pretvara u kilograme po kvadratnom milimetru. Feritni metal šava (WM) ima dobru korelaciju sa Martens tvrdoćom i tvrdoćom po Vickersu ispod 250 HV unutar $\pm 5\%$ ograničenja. Kod većih vrednosti, Martens tvrdoća je niža od tvrdoće po Vickersu, što ukazuje da se ravanski elastični oporavak dogodio u značajnom obimu, nakon uklanjanja ispitne sile čime se smanjuju optički merene dijagonale.

Tvrdoća otisaka (HIT) pokazuje veća odstupanja pri

at low Vickers hardness values. The values are consistently higher than Vickers hardness, following approximately the +5 % line above 200 HV. Due to the good agreement of Martens hardness below 250 HV, it is used for the ferritic samples in the current study.

niskim vrednostima tvrdoće po Vickersu. Vrednosti su konstantno veće od Vickers tvrdoća, nakon otprilike 5% linija iznad 200 HV. Zbog dobrog slaganja Martens tvrdoće 250 HV, ona se koristi za feritne uzorke u studiji

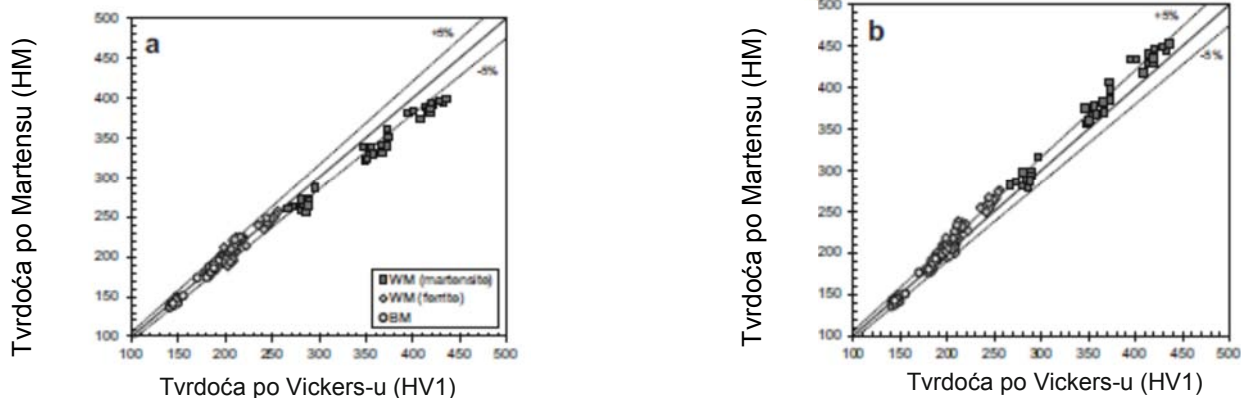


Fig. 14 Comparison of base metal (BM) and weld metal (WM) Vickers hardness (HV1) to a Martens hardness (HM) and b indentation hardness converted to Vickers hardness. The asterisk indicates conversion of units from MPa to kg/mm². The measurements are from Ref. [23], although not presented there in this form

SI. 14 Poređenje Vickers tvrdoća (HV1) sa Martens tvrdoćom (HM) osnovnog materijala (BM) i metala šava (WM) i b tvrdoće otisaka pretvorene u tvrdoću po Vickersu. Zvezdica označava konverziju jedinica iz MPa u kg / mm². Merenja su iz Ref. [23], iako nije ovaj oblik ovde prikazan

Appendix 2: Grain size contour and hardness values

This appendix provides an alternative representation of the grain size contour presented in Fig. 12. In order to reveal the microstructure under each indentation, the hardness indentations have been moved below each indentation in Fig. 15. The measured hardness values are presented in Table 4.

Dodatak 2: Kontura veličine zrna i vrednosti tvrdoće

Ovaj dodatak daje alternativni prikaz veličine zrna konture prikazan na sl. 12. Kako bi se otkrila mikrostruktura pod svakim otiskom, tvrdoća otiska je pomerena ispod svakog otiska sa sl. 15. a izmerene vrednosti tvrdoća prikazane su u tabeli 4.

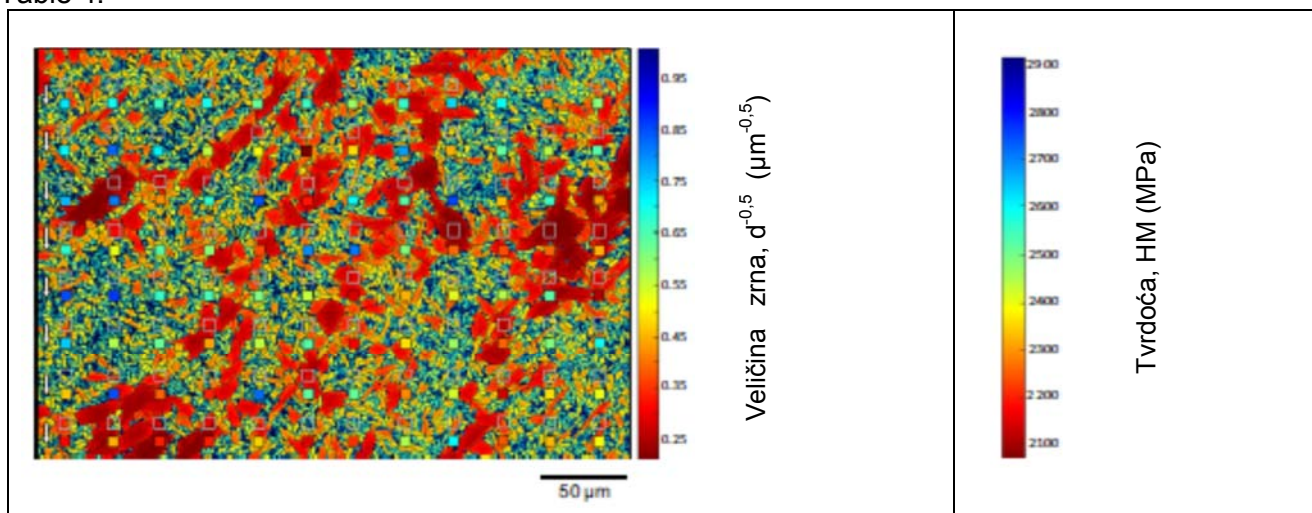


Fig. 15 The hardness value for each indentation overlaid on mean grain size contour for the heterogeneous weld metal area A2. Hardness values are shown below each indentation, indicated by the arrows on the left side, to reveal the grain size under the indentations. The grain size colour contour ranges from 99 to 1 % probability level grain size

SI. 15 Vrednost tvrdoće za svaki otisak preklapljen na konturu srednje veličine zrna za područje heterogenog šava A2. Vrednosti tvrdoća su prikazane ispod svakog otiska, označeno strelicama na levoj strani, da bi se otkrila veličina zrna ispod otiska boja konture veličine zrna kreće se od 99 na 1% veličine nivoa verovatnoće zrna

		Intentionation number											
		1	2	3	4	5	6	7	8	9	10	11	12
Intentionation row	8	2615	2587	2548	2585	2515	2549	2464	2557	2629	2593	2283	2485
	7	2605	2726	2609	2437	2396	2068	2356	2678	2320	2514	2445	2530
	6	2657	2701	2295	2559	2737	2192	2592	2522	2751	2332	2549	2312
	5	2564	2405	2526	2484	2239	2691	2708	2488	2259	2238	2259	2323
	4	2747	2763	2554	2540	2494	2432	2145	2322	2411	2449	2523	2113
	3	2541	2449	2513	2309	2441	2524	2170	2361	2468	2256	2491	2586
	2	2341	2743	2258	2200	2720	2521	2513	2292	2421	2133	2360	2402
	1	2174	2321	2200	2197	2349	2143	2213	2453	2596	2247	2327	2396

Intentionation (1,1) is located in the lower left corner and intentionation (12, 8) in the upper corner of the figures

Table 4. Martens hardness (HM) values [MPa] for the intentionations presented in Figs. 12 i 15

		Broj otiska											
		1	2	3	4	5	6	7	8	9	10	11	12
Niz otisaka	8	2615	2587	2548	2585	2515	2549	2464	2557	2629	2593	2283	2485
	7	2605	2726	2609	2437	2396	2068	2356	2678	2320	2514	2445	2530
	6	2657	2701	2295	2559	2737	2192	2592	2522	2751	2332	2549	2312
	5	2564	2405	2526	2484	2239	2691	2708	2488	2259	2238	2259	2323
	4	2747	2763	2554	2540	2494	2432	2145	2322	2411	2449	2523	2113
	3	2541	2449	2513	2309	2441	2524	2170	2361	2468	2256	2491	2586
	2	2341	2743	2258	2200	2720	2521	2513	2292	2421	2133	2360	2402
	1	2174	2321	2200	2197	2349	2143	2213	2453	2596	2247	2327	2396

Otisak (1,1) je lociran u donjem levom uglu a otisak (12, 8) u gornjem desnom uglu slike

Tabela 4. Vrednosti Martens tvrdoća (MP) [MPa] za otiske prikazane na sl. 12 i 15

Open Access

This article is distributed under the terms of the Creative Commons Attribution 4.0 International License

(<http://creativecommons.org/licenses/by/4.0/>) which permits unrestricted use, distribution, and reproduction in any medium, provided you give appropriate credit to the original author(s) and the source, provide a link to the Creative Commons license, and indicate if changes were made.

Otvoreni pristup

Ovaj članak se distribuira pod uslovima internacionalne licence Creative Commons Attribution 4.0

(<http://creativecommons.org/licenses/by/4.0/>), koji dozvoljava neograničenu upotrebu, distribuciju i reprodukciju u svakom pogledu, uz obezbeđen odgovarajući kredit ka autoru(e)/ime originala, uz obezbeđenje linka sa Creative Commons licencom, gde se navode napravljene izmene.

References

- Hall EO (1954) Variation of hardness of metals with grain size. *Nature* 173:948–9
- Armstrong RW, Codd I, Douthwaite RM, Petch NJ (1962) The plastic deformation of polycrystalline aggregates. *Philos Mag* 7:45–58
- Armstrong RW (1970) The influence of polycrystal grain size on several mechanical properties of materials. *Metall Mater Trans* 1: 1169–76
- Tachibana S, Kawachi S, Yamada K, Kunio T (1988) Effect of grain refinement on the endurance limit of plain carbon steels at various strength levels. *Nippon Kikai Gakkai Ronbunshu, A* Hen/Transactions Japan Soc Mech Eng Part A 54:1956–61
- Furukawa M, Horita Z, Nemoto M, Valiev RZ, Langdon TG (1996) Microhardness measurements and the Hall–Petch relationship in an Al–Mg alloy with submicrometer grain size. *Acta Mater* 44:4619–29. doi:10.1016/1359-6454(96)00105-X
- Chapetti M, Miyata H, Tagawa T, Miyata T, Fujioka M (2004) Fatigue strength of ultra-fine grained steels. *Mater Sci Eng A* 381: 331–6. doi:10.1016/j.msea.2004.04.055
- Hansen N (2004) Hall–Petch relation and boundary strengthening. *Scr Mater* 51:801–6. doi:10.1016/j.scriptamat.2004.06.002

8. Hall EO (1951) The deformation and ageing of mild steel: III discussion of results. *Proc Phys Soc Sect B* 64:747–53
9. Petch NJ (1953) The cleavage strength of polycrystals. *J Iron Steel Inst* 174:25–8
10. Masumura RA, Hazzledine PM, Pande CS (1998) Yield stress of fine grained materials. *Acta Mater* 46:4527–34. doi:10.1016/S1359-6454(98)00150-5
11. Roebuck B (2000) Measurement of grain size and size distribution in engineering materials. *Mater Sci Technol* 16:1167–74
12. Mingard KP, Roebuck B, Quested P, Bennett EG (2010) Challenges in microstructural metrology for advanced engineered materials. *Metrologia* 47:S67–82. doi:10.1088/0026-1394/47/2/S08
13. Mingard KP, Roebuck B, Bennett EG, Gee MG, Nordenstrom H, Sweetman G et al (2009) Comparison of EBSD and conventional methods of grain size measurement of hardmetals. *Int J Refract Met Hard Mater* 27:213–23. doi:10.1016/j.ijrmhm.2008.06.009
14. Mingard KP, Day AP, Quested PN (2014) Recent developments in two fundamental aspects of electron backscatter diffraction. *IOP Conf Ser Mater Sci Eng* 55:012011. doi:10.1088/1757-899X/55/1/012011
15. Mingard KP, Quested PN, Peck MS (2012) Determination of grain size by EBSD - Report on a round robin measurement of equiaxed Titanium
16. ISO (2012) ISO 13067 - Microbeam analysis. Electron backscatter diffraction. Measurement of average grain size
17. Kurzydowski KJ, Bucki JJ (1993) Flow stress dependence on the distribution of grain size in polycrystals. *Acta Metall Mater* 41:3141–6
18. Weertman JR, Sanders PG, Youngdahl CJ (1997) The strength of nanocrystalline metals with and without flaws. *Mater Sci Eng A* 234–236:77–82
19. Morita T, Mitra R, Weertman JR (2004) Micromechanics model concerning yield behavior of nanocrystalline materials. *Mater Trans* 45:502–8. doi:10.2320/matertrans.45.502
20. Berbenni S, Favier V, Berveiller M (2007) Micro-macro modelling of the effects of the grain size distribution on the plastic flow stress of heterogeneous materials. *Comput Mater Sci* 39:96–105. doi:10.1016/j.commatsci.2006.02.019
21. Raeisinia B, Sinclair CW, Poole WJ, Tomé CN (2008) On the impact of grain size distribution on the plastic behaviour of polycrystalline metals. *Model Simul Mater Sci Eng* 16:025001. doi:10.1088/0965-0393/16/2/025001
22. Ramtani S, Bui HQ, Dirras G (2009) A revisited generalized selfconsistent polycrystal model following an incremental small strain formulation and including grain-size distribution effect. *Int J Eng Sci* 47:537–53. doi:10.1016/j.ijengsci.2008.09.005
23. Lehto P, Remes H, Saukkonen T, Hänninen H, Romanoff J (2014) Influence of grain size distribution on the Hall–Petch relationship of welded structural steel. *Mater Sci Eng A* 592:28–39. doi:10.1016/j.msea.2013.10.094
24. Gundersen HJG, Jensen EB (1983) Particle sizes and their distributions estimated from line- and point-sampled intercepts. Including graphical unfolding. *J Microsc* 131:291–310
25. Gundersen HJG, Jensen EB (1985) Stereological estimation of the volume-weighted mean volume of arbitrary particles observed on random sections. *J Microsc* 138:127–42
26. ASTM E1382 - 97 (2004) Standard test methods for determining average grain size using semiautomatic and automatic image analysis. ASTM International, West Conshohocken. doi:10.1520/E1382-97R04
27. Takeuchi S (2001) The mechanism of the inverse Hall–Petch relation of nanocrystals. *Scr Mater* 44:1483–7. doi:10.1016/S1359-6462(01)00713-8
28. Fan G, Choo H, Liaw P, Lavernia E (2005) A model for the inverse Hall–Petch relation of nanocrystalline materials. *Mater Sci Eng A* 409:243–8. doi:10.1016/j.msea.2005.06.073
29. Underwood EE (1970) Quantitative stereology. Addison-Wesley Publishing Co., Reading
30. ASTM E1245 - 03 (2003) Standard practice for determining the inclusion or second-phase constituent content of metals by automatic image analysis. ASTM International, West Conshohocken. doi:10.1520/E1245-03
31. Lehto P (2015) Aalto University wiki - grain size measurement using Matlab. <https://wiki.aalto.fi/display/GSMUM>
32. (1991) Guide to the light microscope examination of ferritic steel weld metals, Doc. IIW IX-1533-88. *Weld World* 29:160–76
33. ASTM E 562 - 02 (2002) Standard test method for determining volume fraction by systematic manual point count. ASTM International, West Conshohocken. doi:10.1520/E0562-11
34. ISO 14577-1 (2002) Metallic materials. Instrumented indentation test for hardness and materials parameters. Part 1: Test method. International Organization for Standardization, Geneva
35. Gee M, Mingard K, Roebuck B (2009) Application of EBSD to the evaluation of plastic deformation in the mechanical testing of WC/Co

hardmetal. *Int J Refract Met Hard Mater* 27:300–12. doi:10.1016/j.ijrmhm.2008.09.003

36. Mingard KP, Roebuck B, Bennett EG, Thomas M, Wynne BP, Palmiere EJ (2007) Grain size measurement by EBSD in complex hot deformed metal alloy microstructures. *J Microsc* 227:298–308. doi:10.1111/j.1365-2818.2007.01814.x

37. Saukkonen T, Aalto M, Virkkunen I, Ehrnstén U, Hänninen H (2011) Plastic strain and residual stress distributions in an AISI 304 stainless steel BWR pipe weld. 15th Int. Conf. Environ. Degrad, p. 2351–67

38. Radwański K, Wrożyna A, Kuziak R (2015) Role of the advanced microstructures characterization in modeling of mechanical properties of AHSS steels. *Mater Sci Eng A* 639:567–74. doi:10.1016/j.msea.2015.05.071

39. Nie W, Shang C, You Y, Zhang X, Subramanian S (2013) Microstructure and toughness of the simulated welding heat affected zone in X100 pipeline steel with high deformation resistance. *Acta Metall Sin* 48:797–806. doi:10.3724/SP.J.1037.2012.00215

40. Sabooni S, Karimzadeh F, Enayati MH, Ngan a HW (2015) Friction-stir welding of ultrafine grained austenitic 304L stainless steel produced by martensitic thermomechanical processing. *Mater Des* 76:130–40. doi:10.1016/j.matdes.2015.03.052

41. Gazder A, Cao W, Davies CHJ, Pereloma EV (2008) An EBSD investigation of interstitial-free steel subjected to equal channel angular extrusion. *Mater Sci Eng A* 497:341–52. doi:10.1016/j.msea.2008.07.030

42. Haušild P, Materna A, Nohava J (2014) Characterization of anisotropy in hardness and indentation modulus by nanoindentation. *Metallogr Microstruct Anal* 3:5–10. doi:10.1007/s13632-013-0110-8

43. Stinville JC, Tromas C, Villechaise P, Templier C (2011) Anisotropy changes in hardness and indentation modulus induced by plasma nitriding of 316L polycrystalline stainless steel. *Scr Mater* 64:37–40. doi:10.1016/j.scriptamat.2010.08.058

44. Patriarca L, Abuzaid W, Sehitoglu H, Maier HJ (2013) Slip transmission in bcc FeCr polycrystal. *Mater Sci Eng A* 588:308–17. doi:10.1016/j.msea.2013.08.050

45. SoerW, De Hosson JTM (2005) Detection of grain-boundary resistance to slip transfer using nanoindentation. *Mater Lett* 59:3192–5. doi:10.1016/j.matlet.2005.03.075

46. Durst K, Backes B, Göken M (2005) Indentation size effect in metallic materials: correcting for the size of the plastic zone. *Scr Mater* 52:1093–7. doi:10.1016/j.scriptamat.2005.02.009

47. Lilleodden E, NixW (2006) Microstructural length-scale effects in the nanoindentation behavior of thin gold films. *Acta Mater* 54:1583–93. doi:10.1016/j.actamat.2005.11.025

48. Zhao MC, Yang K, Shan YY (2003) Comparison on strength and toughness behaviors of microalloyed pipeline steels with acicular ferrite and ultrafine ferrite. *Mater Lett* 57:1496–500. doi:10.1016/S0167-577X(02)01013-3

49. Fattahi M, Nabhani N, Hosseini M, Arabian N, Rahimi E (2013) Effect of Ti-containing inclusions on the nucleation of acicular ferrite and mechanical properties of multipass weld metals. *Micron* 45:107–14. doi:10.1016/j.micron.2012.11.004

50. Seo JS, Lee C, Kim HJ (2013) Influence of oxygen content on microstructure and inclusion characteristics of bainitic weld metals. *ISIJ Int* 53:279–85

51. Seo JS, Kim HJ, Lee C (2013) Effect of Ti addition on weld microstructure and inclusion characteristics of bainitic GMAwelds. *ISIJ Int* 53:880–6. doi:10.2355/isijinternational.53.880

52. Han R, Lu S, Dong W, Li D, Li Y (2015) The morphological evolution of the axial structure and the curved columnar grain in the weld. *J Cryst Growth* 431:49–59. doi:10.1016/j.jcrysgro.2015.09.001

53. Han R, DongW, Lu S, Li D, Li Y (2014) Modeling of morphological evolution of columnar dendritic grains in the molten pool of gas tungsten arc welding. *Comput Mater Sci* 95:351–61. doi:10.1016/j.commatsci.2014.07.052

54. Kidess A, Tong M, Duggan G, Browne DJ, Kenjeres S, Richardson I et al (2015) An integrated model for the post-solidification shape and grain morphology of fusion welds. *Int J Heat Mass Transf* 85:667–78. doi:10.1016/j.ijheatmasstransfer.2015.01.144

55. Kou S, Le Y (1986) Nucleation mechanism and grain refining of weld metal. *Weld J* 65:305–13

56. Tan W, Shin YC (2015) Multi-scale modeling of solidification and microstructure development in laser keyhole welding process for austenitic stainless steel. *Comput Mater Sci* 98:446–58. doi:10.1016/j.commatsci.2014.10.063